# Environmental Security Technology Certification Program
# Final Report - Revision 1

## Project Number UX-0534
## High Density Lidar and Orthophotography in UXO Wide Area Assessment

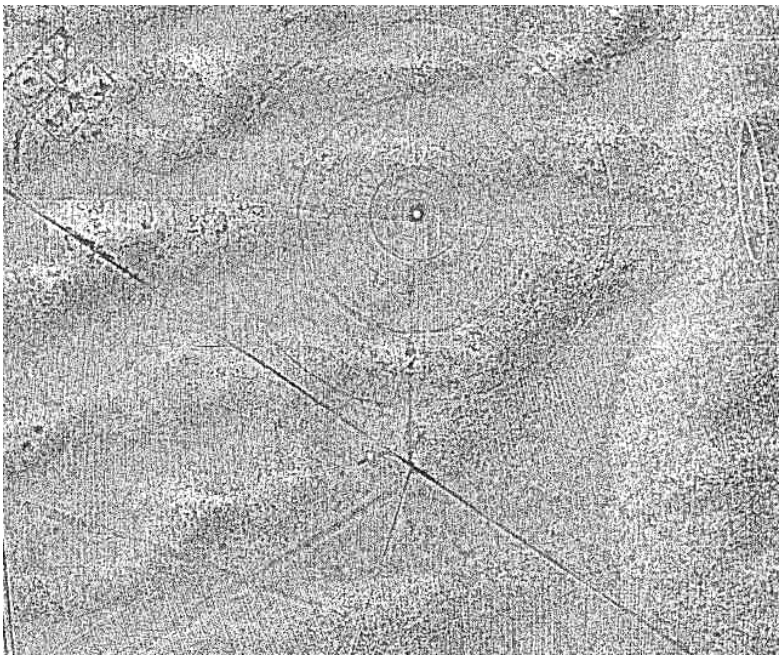

August 2007

Distribution Statement A: Approved for Public Release, Distribution is Unlimited

# CONTENTS

ABBREVIATIONS AND ACRONYMS ..... vii

ACKNOWLEDGEMENTS/ABSTRACT ..... A-1

1.0 INTRODUCTION ..... 1-1
- 1.1 BACKGROUND ..... 1-1
- 1.2 OBJECTIVES OF THE DEMONSTRATION ..... 1-1
- 1.3 REGULATORY DRIVERS ..... 1-2
- 1.4 STAKEHOLDER/END-USER ISSUES ..... 1-2

2.0 TECHNOLOGY DESCRIPTION ..... 2-1
- 2.1 TECHNOLOGY DEVELOPMENT AND APPLICATION ..... 2-1
  - 2.1.1 Technology Background ..... 2-1
- 2.2 PREVIOUS TESTING OF THE TECHNOLOGY ..... 2-3
- 2.3 FACTORS AFFECTING COST AND PERFORMANCE ..... 2-4
- 2.4 ADVANTAGES AND LIMITATIONS OF THE TECHNOLOGY ..... 2-5

3.0 DEMONSTRATION DESIGN ..... 3-1
- 3.1 PERFORMANCE OBJECTIVES ..... 3-1
- 3.2 SELECTION OF TEST SITES ..... 3-1
- 3.3 TEST SITE HISTORY, CHARACTERISTICS AND PRESENT OPERATIONS ..... 3-1
- 3.4 PRE-DEMONSTRATION TESTING AND ANALYSIS ..... 3-4
  - 3.4.1 Kirtland Demonstration Site ..... 3-4
  - 3.4.2 Victorville Demonstration Site ..... 3-5
- 3.5 TESTING AND EVALUATION PLAN AND PROCEDURES ..... 3-7
  - 3.5.1 Demonstration Set-Up and Start-Up ..... 3-7
  - 3.5.2 Period of Operation and Area Characterized ..... 3-7
  - 3.5.3 Demobilization ..... 3-8
- 3.6 SELECTION OF ANALYTICAL/TESTING METHODS ..... 3-8
- 3.7 RESULTS ..... 3-9
  - 3.7.1 Data Collection ..... 3-9
  - 3.7.2 Safety Issues ..... 3-10
  - 3.7.3 Data Processing Steps ..... 3-10
  - 3.7.4 Detection and Delineation of Munitions Response Sites ..... 3-12
  - 3.7.5 Kirtland – Target N3 Results ..... 3-13
  - 3.7.6 Kirtland – Target N2 Results ..... 3-15
  - 3.7.7 Kirtland – Target NDIA Results ..... 3-16
  - 3.7.8 Kirtland – Target SORT Results ..... 3-18
  - 3.7.9 Kirtland – Other Sites of Interest ..... 3-18
  - 3.7.10 Victorville – Target DBT Y Results ..... 3-19

**CONTENTS (Continued)**

3.7.11 Victorville – Target PBR 15 Results ..... 3-20
3.7.12 Detection of Potential Munitions-Related Ground Features ..... 3-21
3.7.13 Data Density Effects - General Results ..... 3-24
3.7.14 Data Density Effects - Quantitative Results ..... 3-28
3.7.15 Flight Line Orientation Effects ..... 3-31
3.7.16 Data Artifacts and Noise Effects ..... 3-32
3.7.17 Vegetation Patterns ..... 3-34
3.7.18 Lidar and Orthophoto Positional Accuracy ..... 3-35
3.7.19 Other Observations ..... 3-37

4.0 PERFORMANCE ASSESSMENT ..... 4-1
4.1 PERFORMANCE CRITERIA ..... 4-1
4.2 PERFORMANCE CONFIRMATION METHODS ..... 4-17
4.2.1 Demonstration-Level Confirmation Methods ..... 4-17
4.2.2 Program Level Confirmation Methods ..... 4-17
4.2.3 Results: Kirtland ..... 4-18
4.2.4 Results: Victorville ..... 4-26
4.2.5 Findings and Conclusions ..... 4-28
4.3 DATA ANALYSIS, INTERPRETATION, AND EVALUATION ..... 4-29
4.3.1 Correlations with Operating Parameters and Required Performance Specifications ..... 4-29
4.3.2 Optimum Operating Conditions and Appropriate Uses of the Technologies ..... 4-30

5.0 COST ASSESSMENT ..... 5-1
5.1 COST REPORTING ..... 5-1
5.2 COST ANALYSIS ..... 5-2
5.2.1 Cost drivers ..... 5-2
5.2.2 Cost Sensitivities and Additional Potential Savings ..... 5-3
5.3 COST COMPARISON ..... 5-3

6.0 IMPLEMENTATION ISSUES ..... 6-1
6.1 ENVIRONMENTAL CHECKLIST ..... 6-1
6.2 OTHER REGULATORY ISSUES ..... 6-1
6.3 END-USER ISSUES ..... 6-1

7.0 REFERENCES ..... 7-1

## CONTENTS (Continued)

### APPENDICES

A Lidar and Orthophoto Positional Accuracy Results
B Combining Lidar Data from Multiple Flights
C Variation in Lidar Data Density and Potential Effect on Feature Identification
D GIS-Based Methods for Creating Ground Surface Models from Lidar Points
E Automation of Lidar Data Processing in the ESRI GIS Environment
F Analytical Methods Supporting Experimental Design
G Quality Assurance Project Plan
H Health and Safety Plan
I Points of Contact

## CONTENTS (Continued)

### FIGURES

Figure 2-1 Helicopter-Mounted Lidar and Orthophoto Sensor Equipment ..... 2-1
Figure 2-2 Lidar System Operations ..... 2-2
Figure 3-1 Kirtland Precision Bombing Range Site ..... 3-2
Figure 3-2 Victorville DBT Y and PBR Target 15 Site ..... 3-3
Figure 3-3 Kirtland Control Points ..... 3-4
Figure 3-4 Kirtland Test Craters ..... 3-5
Figure 3-5 Victorville Control Points ..... 3-6
Figure 3-6 Victorville Test Craters ..... 3-6
Figure 3-7 Lidar Equipment Setup ..... 3-7
Figure 3-8 Kirtland Sample Flight Lines ..... 3-9
Figure 3-9 Victorville Sample Flight Lines and Example Image ..... 3-10
Figure 3-10 Target N3 Elements ..... 3-14
Figure 3-11 Target N2 Orthophoto and Lidar ..... 3-16
Figure 3-12 Target NDIA Orthophoto and Lidar ..... 3-17
Figure 3-13 Target SORT Orthophoto ..... 3-18
Figure 3-14 Sample Additional Sites of Interest ..... 3-19
Figure 3-15 Target DBT Y Orthophoto and Lidar ..... 3-20
Figure 3-16 Target PBR 15 Orthophotos, Lider Surface Model and Lidar Intensity Image ..... 3-21
Figure 3-17 Kirtland Target NDIA Potential Crater Detection ..... 3-22
Figure 3-18 Victorville Target DBT/Craters, Orthophotos and Lidar ..... 3-22
Figure 3-19 Victorville Target DBT Y - MRS Boundaries ..... 3-23
Figure 3-20 Kirtland Test Craters, Orthophotos ..... 3-24
Figure 3-21 Kirtland Test Craters, Lidar Surface Models ..... 3-25
Figure 3-22 Victorville Test Craters, Lidar Surface Models ..... 3-27
Figure 3-23 Kirtland Sample Features of Interest ..... 3-28
Figure 3-24 Kirtland Area Features by Data Source ..... 3-29
Figure 3-25 Kirtland Line Feature Length by Data Source ..... 3-30
Figure 3-26 Victorville Features by Data Source ..... 3-31
Figure 3-27 Kirtland Flightline Orientation Effects ..... 3-32
Figure 3-28 Kirkland Flight Line Data Overlap Effect ..... 3-33
Figure 3-29 Victorville Lidar “Corduroy” Effect ..... 3-34
Figure 3-30 Kirtland Vegetation Patterns ..... 3-35
Figure 3-31 Use of Orthophotos to Resolve Apparent Lidar Data Discrepancy ..... 3-37
Figure 4-1 Kirtland Helicopter Magnetometry Density Grid ..... 4-18
Figure 4-2 Kirtland Target N3 and Associated AOIs ..... 4-20
Figure 4-3 Kirtland Target N3 and Associated AOIs, Geophysics Data ..... 4-21
Figure 4-4 Kirtland Target SORT, Geophysics Data ..... 4-22
Figure 4-5 Kirtland Target SORT, Intrusive Investigation Results ..... 4-23

## CONTENTS (Continued)

Figure 4-6 Kirtland Target N2, Geophysics Data ..... 4-24
Figure 4-7 Kirtland Target NDIA, Geophysics Data ..... 4-25
Figure 4-8 Victorville Filtered Geophysics Data ..... 4-27
Figure 4-9 Victorville Helicopter Magnetometry Density Grid ..... 4-28

## CONTENTS (Continued)

## TABLES

2-1 Cost and Performance Factors ..... 2-4
2-2 Technology Advantages and Limitations ..... 2-5
3-1 Data Collection Periods ..... 3-8
3-2 MRS Detection – Kirtland ..... 3-12
3-3 Target N3 Detection Results ..... 3-13
3-4 Target NDIA Detection Results ..... 3-17
3-5 Achieved Lidar Data Densities ..... 3-25
3-6 Kirtland Potential Features ..... 3-29
3-7 Victorville Potential Features ..... 3-30
3-8 Overall Positional Accuracy Results ..... 3-36
4-1 Performance Criteria ..... 4-1
4-2 Data Quality Metrics—MRS Identification and Analysis ..... 4-2
4-3 Data Quality Metrics, Individual Performance Measures ..... 4-8
5-1 Actual and Projected Costs ..... 5-1

# ABBREVIATIONS AND ACRONYMS

| | |
|---|---|
| AOI | area of interest |
| CERCLA | Comprehensive Environmental Response, Compensation, and Liability Act |
| CSM | conceptual site model |
| DBT | Demolition Bombing Target |
| DEM | digital elevation model |
| DoD | Department of Defense |
| EM | electromagnetic |
| EMI | electromagnetic induction |
| ESTCP | Environmental Security Technology Certification Program |
| GIS | Geographical Information System |
| GPS | Global Positioning System |
| HE | high explosive |
| IMU | Inertial Measurement Unit |
| lidar | light detection and ranging |
| MEC | munitions and explosives of concern |
| MRS | munitions response site |
| NDIA | New Demolitions Impact Area |
| PBR | Precision Bombing Range |
| QA | quality assurance |
| QC | quality control |
| SAR | synthetic aperture radar |
| SORT | Simulated Oil Refinery Target |
| TIN | Triangulated Irregular Network |
| TRSI | Terra Remote Sensing, Inc. |
| UXO | unexploded ordnance |
| WAA | wide area assessment |

## ACKNOWLEDGEMENTS

This project was made possible through funding provided by the Environmental Security Technology Certification Program (ESTCP). We express our sincere appreciation to Dr. Jeffrey Marqusee, ESTCP Program Director, and Dr. Anne Andrews, Unexploded Ordnance (UXO) Program Manager, as well as Dr. Herb Nelson of the Naval Research Lab, the project manager for the Wide Area Assessment Pilot Program, for their support and guidance to URS for this project. We would also like to express our thanks to ESTCP's support staff at Versar, Inc. and HGL Inc., and to the contract staff at the US Army Corps of Engineers Humphreys Engineering Center.

Grateful acknowledgement is also made to our demonstration partner Terra Remote Sensing, Inc. of Sydney, British Columbia, who performed lidar and orthophoto data acquisition and contributed significantly to development of data analysis and quality assurance/quality control methods.

## ABSTRACT

URS Corporation and Terra Remote Sensing, Inc. were awarded ESTCP funding to demonstrate the utility of high-density lidar and orthophotography as one component of a multi-technology approach to UXO/munitions and explosives of concern (MEC) Wide Area Assessment (WAA). Lidar and orthophotography were collected at two former military sites: the 5,000-acre Kirtland Precision Bombing Range site near Albuquerque, New Mexico, and the 5,640 Victorville Demonstration Bombing Target (DBT) Y site near Victorville, California. Data was collected at the Kirtland site over three days in August 2005 and at the Victorville site over two three-day periods in January and February 2006.

Performance objectives of the demonstration were to:

- Identify munitions response sites (MRS) such as bombing targets, open burn/open detonation areas, and burial pits that are the result of sanctioned military activities (whether documented or undocumented) that could reasonably be expected to result in the release of MEC to the environment

- Provide information about the site and the MRS to support future investigation, prioritization, and cost estimation

- For areas outside of the MRS, provide information to support regulatory decisions regarding the portions of the munitions response areas outside of the MRS, including

decisions as to requirements for further investigation, institutional controls, or no further action

- Describe the certainty associated with the initial conceptual site model (CSM), and examine the incremental contributions of each technology to improvements in that certainty

These objectives were met. The MRS and munitions-related features were successfully identified, and findings were used to verify and correct the initial CSM. Information from the demonstration was successfully used by subsequent demonstrators and ESTCP in subsequent phases of the WAA Pilot Program. All data accuracy specifications were met. The demonstration provided important insights regarding the appropriate uses and confidence levels for both lidar and orthophoto technologies.

At the Kirtland site, all four of the known targets from the CSM were identified using lidar data. Additionally, three sub-target areas and 16 additional areas of interest were identified, including a potential bull's-eye target ring not documented in the CSM. The areas of interest consisted of isolated groups of potential craters.

Bombing targets at the Kirtland site were constructed from berms; these had weathered to between 5 cm and 15 cm (2 and 7 inches) in height, and most were not visible to ground crews on the site. These targets were clearly visible in the lidar data but generally not in the orthophotos. However, the orthophotos did show some target elements, such as target cross-hairs, that were not visible in the lidar data.

Subsequent validation activities using magnetometry and intrusive investigation verified the bombing targets and the three ancillary target areas, and indicated that the 16 additional areas of interest likely were not munitions-related. Validation activities also showed the presence of two areas of concentrated munitions-related scrap near one of the targets that were not revealed by either the lidar or orthophoto data.

At the Victorville site, both targets identified in the initial CSM were visible in both the lidar and orthophoto data. Large craters were visible in and near DBT Y, the Means Dry Lake bed. Potential craters ranged from 5 to 8 m in diameter and up to 1 m deep. Potential crater locations were used to modify the boundary of the MRS presented in the CSM. Target PBR 15, a bull's-eye target used for precision bombing practice, consisted of a series of rings constructed from asphalt. The target area was clearly visible in the orthophoto and lidar intensity data, and showed no evidence of craters.

Increasing the lidar data density increased the rate of detection of craters in the 1 m to 3 m size range substantially, but had only a weak effect on detection of larger craters, additional areas of interest, and bombing targets. Lidar density effects were most pronounced between the

1.5 pts./$m^2$ data and the 4.5 pts./$m^2$ data sets, and diminished thereafter. Detection of faint linear features was affected by flight line orientation. Common lidar surface artifacts were encountered, consisting of faint lines approximately 0.5 m in height.

The probability of detection for the bombing targets at both sites was 100%, with all of the known targets from the CSM being detected at both sites. Nevertheless, MRS at the Kirtland site were missed: validation activities revealed two sites with concentrated ordnance-related scrap that were not identified using either lidar or orthophotos, presumably because they left little or no surface disturbance. No clear false alarms were encountered for bombing targets. There was no attempt to measure false alarm rates for individual potential craters.

Overall costs for acquisition and processing of lidar and orthophotos were approximately $48/acre for Kirtland and $27/acre for Victorville. Per-acre costs at Kirtland were higher due to acquisition of four lidar flights and two orthophoto sets, compared to two lidar flights and one orthophoto set at Victorville. Costs are projected to be approximately $20/acre for an 18,000-acre site, based on preliminary results from the Former Camp Beale site acquired in late 2006. Costs are projected at between $12 and $14/acre for sites in the 50,000 – 110,000 acre range. Costs for competing technologies are discussed in the Final Report for the WAA Pilot Program.

The results of the demonstration support the use of lidar and orthophotos as an integral part of the WAA Process. These technologies proved to be a cost-effective and reliable means to characterize the sites, validate and correct the initial CSMs, and provide data to focus the application of subsequent methods of investigation. Lidar and orthophotos will not detect sites where there are no surface indications. Consequently, use of lidar and orthophotos should be followed by technologies that detect munitions components directly.

# 1.0 INTRODUCTION

## 1.1 BACKGROUND

Many millions of acres of Department of Defense (DoD) lands are potentially contaminated with military munitions or their components. On the majority of these sites, munitions are concentrated in specific ranges and training areas, while the remainder of the site is ordnance-free. Contaminated sites traditionally have been very expensive to investigate and remediate because of the nature of the contamination and the relatively few innovative approaches available to date.

The current demonstration was conducted as part of the Environmental Security Technology Certification Program (ESTCP) Wide Area Assessment (WAA) Pilot Program, which explored the use of an integrated suite of airborne and ground-based technologies as a means to identify and validate pilot WAA technologies and approaches. Light detection and ranging (lidar) and orthophotography, the subjects of this demonstration, were used in conjunction with synthetic aperture radar (SAR), hyperspectral sensing, helicopter-based magnetometry, and towed-array magnetometry and electromagnetic induction (EMI), along with statistical modeling, in an integrated Geographical Information System (GIS)-based analytical environment.

This report discusses the results of lidar and orthophoto data collection and analysis at two demonstration sites. The results from the WAA Pilot Program as a whole, and the relationship of these two technologies to the entire suite of technologies tested, are discussed in the final report for the WAA Pilot Program as a whole.

## 1.2 OBJECTIVES OF THE DEMONSTRATION

The objective of the demonstration was to demonstrate and validate the ability of lidar and orthophotos to contribute to the WAA process by:

- Identifying munitions response sites (MRS) such as bombing targets, open burn/open detonation areas, and burial pits that are the result of sanctioned military activities (whether documented or undocumented) that could reasonably be expected to result in the release of munitions and explosives of concern (MEC) to the environment

- Providing information about the site and the MRS to support future investigation, prioritization, and cost estimation

- For areas outside of the MRS, providing information to support regulatory decisions, including decisions as to requirements for further investigation, institutional controls, or no further action

- Describing the certainty associated with the initial conceptual site model (CSM), and examining the incremental contributions of each technology to improvements in that certainty

An additional objective was to develop information about the factors that would affect the cost and performance of both technologies, including the relationship between levels of effort and confidence in conclusions. Data density was the primary performance factor tested.

## 1.3 REGULATORY DRIVERS

MEC remediation is generally conducted under authority of the Comprehensive Environmental Response, Compensation, and Liability Act (CERCLA). With many millions of acres of land potentially contaminated with MEC, estimates of the cost of elimination of environmental liability under this statute at known and former DoD sites range as high as several hundred billion dollars. These potentially high costs have led to interest in the development of innovative investigative or screening methods, in order to reduce the costs of conducting WAA and associated remediation activities.

## 1.4 STAKEHOLDER/END-USER ISSUES

The demonstration showed that both lidar and orthophotos can contribute to the WAA process through cost-effective delineation of MRS- and MEC-related features. The demonstration results indicate that lidar and orthophotos are most appropriately used during the early phases of the WAA process, in order to focus and prioritize the subsequent application of more expensive low-altitude and ground-based technologies.

# 2.0 TECHNOLOGY DESCRIPTION

## 2.1 TECHNOLOGY DEVELOPMENT AND APPLICATION

### 2.1.1 Technology Background

Lidar is a well-established airborne technology for modeling ground surfaces. Topographic lidar was first developed in the late 1960s and early 1970s, and has been used for terrain profiling since the mid-1980s. Lidar has been in wide commercial use since around 1993, and the accuracies and limitations of lidar for surface modeling are well documented.

Lidar uses the time of return for a laser pulse to be reflected back to the sensor to measure the elevation of the point of reflection. Use of Global Positioning System (GPS) and Inertial Measurement Unit (IMU) technology to locate the sensor precisely in the air allows for the accurate calculation of the point of reflection of the laser signal from the ground, buildings or vegetation. Multiple returns from a single laser pulse can be detected, increasing the chance of sampling the ground surface through gaps in vegetation. Once elevation data is collected in the form of lidar points, surface models are created and analyzed. The surface modeling process is typically conducted using standard GIS software and methods, and much of the process can be successfully automated. Lidar vendors typically guarantee a vertical accuracy of 0.15 m and a horizontal accuracy of 0.3–0.75 m.

**Figure 2-1**
**Helicopter-Mounted Lidar and Orthophoto Sensor Equipment**

**Figure 2-2**
**Lidar System Operations**

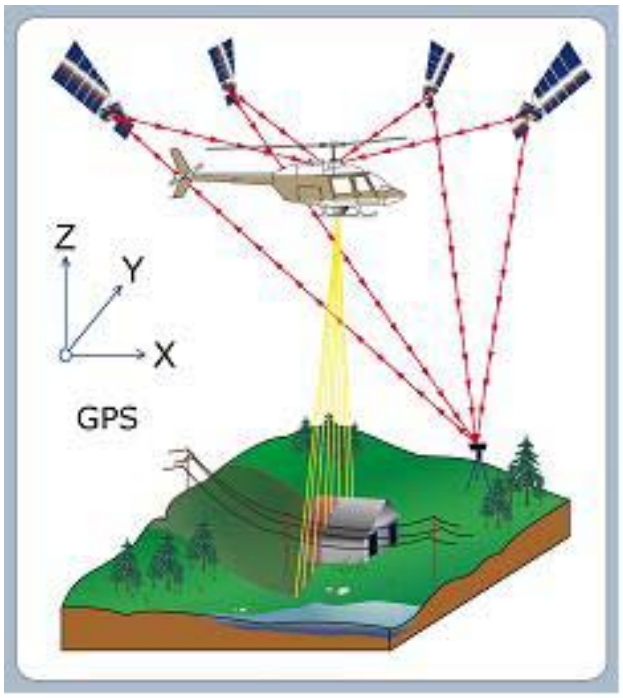


The development of higher-speed (50–100 kHz) laser scanners beginning around 2002 has significantly improved the ability of lidar to locate small features. Currently, high-speed lidar systems are being used to characterize objects in the sub-meter range, such as power line insulators. The accuracy and data density of current lidar systems suggest that the technology could be used to detect ground features indicative of ordnance use, including targets and craters, and that the presence of these features could in turn be used to develop more accurate locations of MEC.

Digital orthophotography has been commercially available since the early 1980s, with steady improvement in the resolution (i.e., pixel size) and precision (i.e., pixel placement) of the images as the technology of digital cameras, GPS, and IMU systems has advanced. Since the mid 1990s, image size has advanced from 1,500 pixels across an image to 4,500 pixels. This has allowed for increased flying heights and a reduced number of images for a given area, with consequent cost savings. Commensurate with this improvement has been a twofold increase in the accuracy of the IMU, allowing for accurate positioning of image pixels at a higher flying height.

Airborne digital cameras have been successfully integrated with lidar sensors. Cameras with an image density of roughly 4,000 x 4,000 pixels are generally favored, because the width of the images collected is very similar to that of the typical lidar point swath. Once collected, individual digital images are mosaiced and color balanced, and the resulting composite image is orthorectified using the lidar data. Orthorectification allows for the accurate location of each photo pixel, eliminating distortion caused by camera angle and topography. Vendors generally guarantee a horizontal accuracy of 3 pixel widths compared to ground control for orthophotography.

Digital images are collected concurrently with lidar and, because the two sensors use the same GPS and IMU, the two data sets can be integrated very accurately. Vendors generally guarantee spatial integration of orthophotos and lidar within 2 pixel widths. Final orthophoto pixel size depends on the flight altitude and the camera specifications; helicopter-based cameras flying at altitudes of 400–450 meters are capable of pixel sizes of approximately 10 cm. Smaller pixel sizes than this are generally impractical due to the low flight elevations and slow flight speeds required to collect properly overlapping images, and the very large numbers of images that would need to be mosaiced.

The ability to produce spatially accurate orthophotos with relatively small pixel sizes suggests that this technology could be used to identify ordnance-related features, and to cross-validate technologies such as lidar.

## 2.2 PREVIOUS TESTING OF THE TECHNOLOGY

URS and Terra Remote Sensing, Inc. (TRSI) conducted a successful demonstration of lidar and high-resolution digital imagery at an operational US Navy range near Boardman, Oregon during November 2004. Both the lidar data and the orthophotos were successful in detecting patterns of surface disturbance indicative of unexploded ordnance (UXO)/MEC activities. Moreover, the two data sets were found to complement each other well, each revealing features that the other did not. Orthophotos collected during the November 2004 test flight showed color variations that could not be detected by lidar (for example, painted truck tires used to outline bombing targets). Very subtle ground features, such as vehicle tracks, which were beyond the resolution of the lidar data at that resolution, were visible in the photos.

Even though the lidar data was collected at relatively low density, lidar revealed depressions such as craters better than the orthophotos, where it was difficult to distinguish depressions from shadows or mounds. Lidar was very successful at locating target features such as bull’s-eye rings. Disposal craters could be distinguished from bombing practice craters by their patterns on the ground. Surface models created from lidar data could be analyzed in ways that orthophoto data could not be, such as measuring the depth of craters.

## 2.3 FACTORS AFFECTING COST AND PERFORMANCE

Factors affecting cost and performance of lidar and orthophotos are detailed in Table 2-1.

**Table 2-1**
**Cost and Performance Factors**

| Item | Cost and Performance Factors |
|---|---|
| Lidar data density | Higher lidar data density is generally more expensive, due to the need to acquire and process additional flight lines. |
| Orthophoto data density | Orthophotos with smaller pixels are more expensive, because of the additional flight lines required and the larger number of individual digital images that must be processed and mosaiced. |
| Accuracy and precision requirements | Accuracy and precision are largely determined by the equipment used and the care of the operators. Projects with extremely high accuracy requirements, such as creation of contour lines under 1-foot intervals, can only be accomplished by vendors with extremely new equipment, at higher cost. |
| Site location and logistics | Sites with longer flying times to an airport will be more expensive, as they will require either longer flight times or placing fuel on the test site. |
| Accuracy verification requirements | Verification of accuracy and precision is accomplished through placement of survey control points and comparison of lidar and orthophoto data to those points. Projects with higher verification requirements will be more costly, although this factor is small compared to other factors. |
| Site size | Larger sites can achieve substantial cost savings through amortization of fixed costs, such as mobilization and project planning, as well as through increased efficiency in data acquisition and processing. |
| Vegetation conditions | More densely vegetated sites will have higher costs due to the requirement for additional lidar passes to achieve sufficient point density at the ground surface. Vegetation will affect the ability of both lidar and orthophotos to view or model the ground surface. |
| Permitting and site access | Some DoD sites contain high-security areas, which can present higher costs for pre-flight planning and data collection. These costs result from restrictions on site access, time to acquire needed clearances, and longer flight times to avoid restricted areas.<br>Sites with environmental constraints do not normally impose higher costs for lidar and orthophotography, due to the airborne nature of the technologies. However, the presence of sensitive species may affect pre-flight planning and scheduling (and thus costs) for projects that require landing to re-fuel on the site. |

## 2.4 ADVANTAGES AND LIMITATIONS OF THE TECHNOLOGY

Advantages and limitations offered by use of lidar and orthophotos compared to the traditional approaches to MRS investigation as shown on Table 2-2.

**Table 2-2**
**Technology Advantages and Limitations**

| Item | Advantages |
|---|---|
| Rate of coverage | In an operational setting, data collection rates of 5,000 acres per day can be expected for lidar and orthophotos. This compares favorably to maximum collection rates of around 500 acres per day for helicopter-based magnetometry, and 20 acres per day for towed-array magnetometry. |
| Ability to delineate MRS and MEC-related features | Lidar and orthophotography successfully revealed MRS and MEC-related surface features at both demonstration sites, even many years after their last use. In the case of the Kirtland site, these features were often not visible to observers on the ground. |
| Enhanced planning and risk assessment | Because they can cover entire sites relatively quickly and at lower cost, these technologies can be used to locate and prioritize appropriate areas for use of more costly ground-based technologies. |
| Other benefits | Both technologies provide highly detailed topographic data that can be integrated into a facility's CAD or GIS system and used in subsequent phases of site investigation, site remediation, and range management |
| **Item** | **Limitations** |
| MEC detection | Neither lidar nor orthophotography can directly detect small dimension shell casings or other MEC components. Consequently, further investigation with magnetometers or electromagnetic (EM) sensors is generally required. |
| Elevation data | Orthophotos do not contain elevation information. In practice, it is sometimes difficult to distinguish small surface depressions from small mounds or shadows using orthophotos alone. |
| Vegetation effects | Since both lidar and orthophotos are light-based technologies, neither will penetrate vegetation. Orthophotos do not "look through" vegetation, and lidar point densities will be lower in vegetated areas. However, lidar is frequently successful in penetrating small openings between and within vegetation, and this success has increased with the speed of lidar sensors and the development of the ability to measure multiple returns. |

# 3.0 DEMONSTRATION DESIGN

## 3.1 PERFORMANCE OBJECTIVES

The primary performance objectives for these technologies were to:

- Clarify whether and to what extent lidar and orthophotos can delineate MRS boundaries and MEC-related features, and contribute to focusing and prioritizing subsequent low-altitude and ground-based work

- Reveal relationships between the density of lidar and orthophoto data, their levels of cost, and their ability to accurately locate MRS boundaries and MEC-related ground features

- Clarify whether and to what extent lidar and orthophotos can verify, reveal errors in, or improve the accuracy of the initial CSM

- Contribute data and analysis to the overall combination of technologies used in the WAA Pilot Program, in a manner that is timely to the application of the other technologies demonstrated, in formats useable by other demonstrators, and with sufficient positional accuracy compared to project control points to allow meaningful coordination and comparison

Specific performance criteria and performance metrics related to each of these objectives are established in the Technology Demonstration Plan for each site.

## 3.2 SELECTION OF TEST SITES

Both demonstration sites were chosen by the ESTCP Program Office. Details of the site selection process can be found in the final report for the WAA Pilot Program.

## 3.3 TEST SITE HISTORY, CHARACTERISTICS AND PRESENT OPERATIONS

The first demonstration site was located at the Kirtland Air Force Base Precision Bombing Range (PBR) located approximately 10 miles west of Albuquerque, New Mexico (Figure 3-1). The site is part of a much larger set of bombing ranges used for training purposes during World War II. The study site consisted of approximately 5,120 acres within the PBR located in two parcels to the north and south of the Double Eagle Airport, the primary small aircraft airport for the Albuquerque area. The study area itself is currently undeveloped, although portions are

planned for commercial or industrial development, and airport expansion into the study are is possible.

**Figure 3-1**
**Kirtland Precision Bombing Range Site**

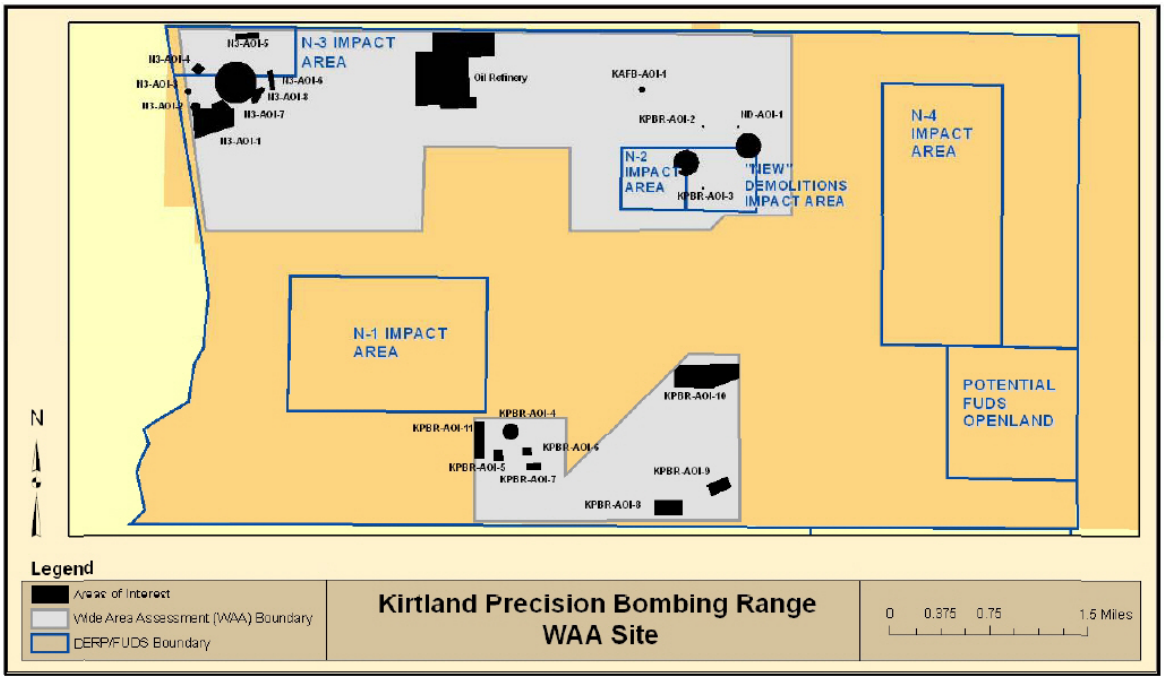


Source: ESTCP (2007a)

Munitions known or suspected to have been used at the site include 100-point practice bombs and 250-pound high explosive (HE) bombs. A certificate of clearance has been issued for one portion of the site, Target N3. Four target areas were identified in the initial CSM as within the study site:

- Target N-2, a 1,000-foot-diameter bull's-eye target used for 100-pound practice bombs
- Target N-3, a 1,000 -foot-diameter bull's-eye target used for 100-pound practice bombs and for scrap storage
- The New Demolitions Impact Area (NDIA), a 1,000 -foot-diameter HE bull's-eye target

- The Simulated Oil Refinery Target (SORT), a target consisting of 350-foot x 350-foot rectangular cells

Locations were given for the first three targets in the CSM. The approximate location of the SORT was given as "somewhere northwest of the Double Eagle airport."

The second demonstration site was located at the Former Victorville Army Air Force Demolition Bombing Target (DBT) Y and PBR 15 (Figure 3-2). The site is located in San Bernardino County, California, approximately 42 miles southeast of the town of Victorville, California. This site lies within a much larger complex of approximately 23 targets used between 1942 and 1945. The site is managed by the US Bureau of Land Management, and is used primarily as a recreation area for off-road vehicles, camping, and target shooting. The demonstration site encompasses approximately 5,640 acres.

**Figure 3-2**
**Victorville DBT Y and PBR Target 15 Site**

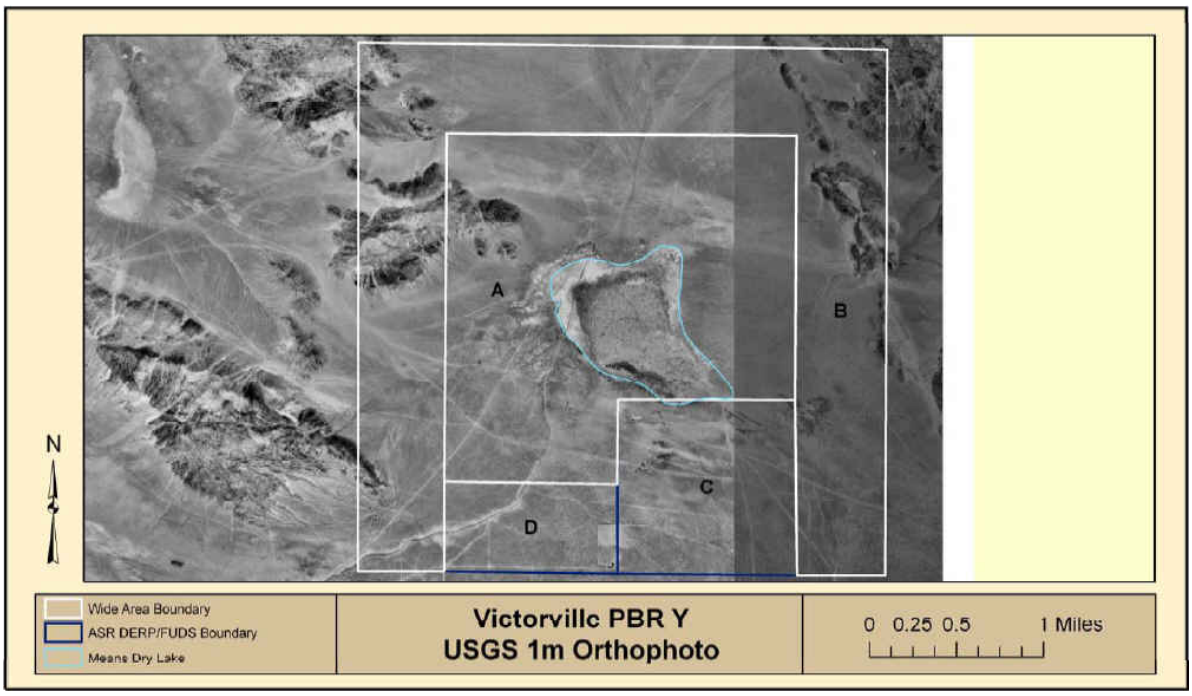


Source: ESTCP (2007b)

Two target areas were identified in the initial CSM for the Victorville site:

- Target DBT Y, located in Means Dry Lake bed in the center of the demonstration site, identified as a demolition bomb target area where bombs between 100 and 2,000 pounds were used.

- Target PBR 15, a suspected bull's-eye target located in the southeast portion of the demonstration site used for precision bombing practice. According to the initial CSM, PBR 15 was not visited during the archival search report site visit and little is known about the area.

## 3.4 PRE-DEMONSTRATION TESTING AND ANALYSIS

### 3.4.1 Kirtland Demonstration Site

Prior to mobilization, ESTCP established five survey control points on the Kirtland site (Figure 3-3). TRSI established four additional control points and independently occupied two of the ESTCP control points. Six vertical control structures were placed adjacent to the six control points established by TRSI, but two were vandalized prior to data collection. A test crater area was established in the south portion of the project site containing two test craters at 1.5 m diameter, two at 1.0 m diameter, and six at 0.32 m diameter (Figure 3-4).

**Figure 3-3**
**Kirtland Control Points**

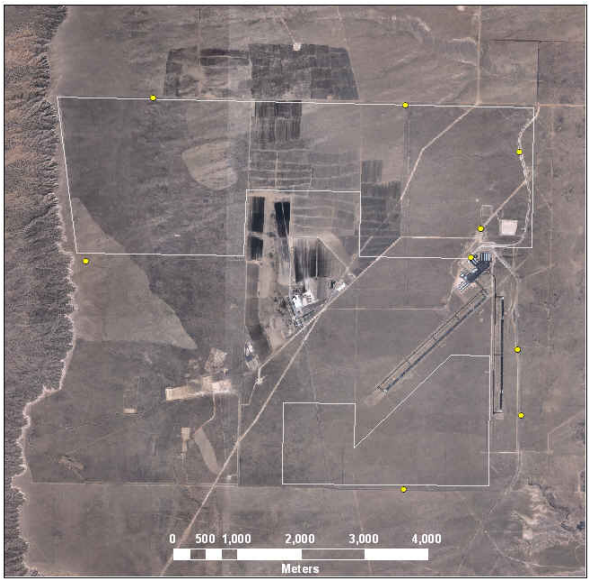


Control point locations

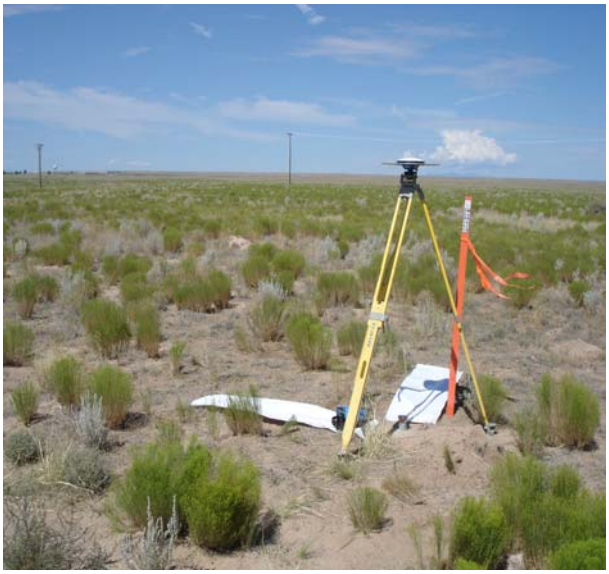

Example Kirtland control point

**Figure 3-4**
**Kirtland Test Craters**

0.32 m test craters

1.5 m test crater

On August 9, 2005, calibration flights were conducted to establish appropriate pitch, yaw, and roll correction factors and appropriate lidar sensor speeds. A laser pulse rate of 50 kHz was selected, based on performance at a variety of speeds tested. Lidar and orthophoto missions began the same day.

### 3.4.2 Victorville Demonstration Site

At the Victorville site, TRSI established eight survey control points on the site (Figure 3-5). These sites were later independently occupied by ESTCP. Four vertical control structures and 10 test craters were also established, at the same sizes as for the Kirtland site (Figure 3-6). Unlike at Kirtland, the Victorville test craters were not grouped together in one location. This revised configuration eliminated the observed tendency to infer the location of smaller test craters from the known location of the adjacent larger craters.

**Figure 3-5**
**Victorville Control Points**

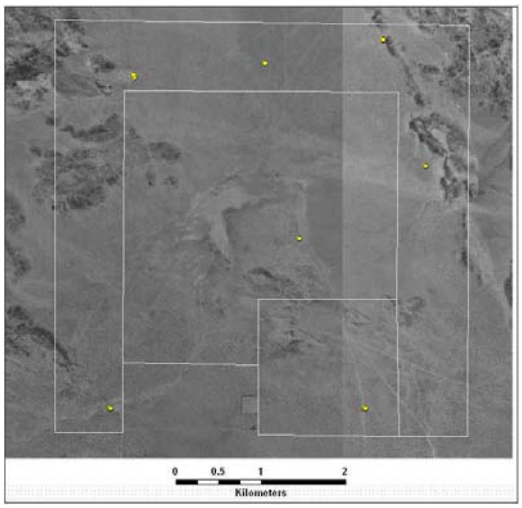


Control point locations

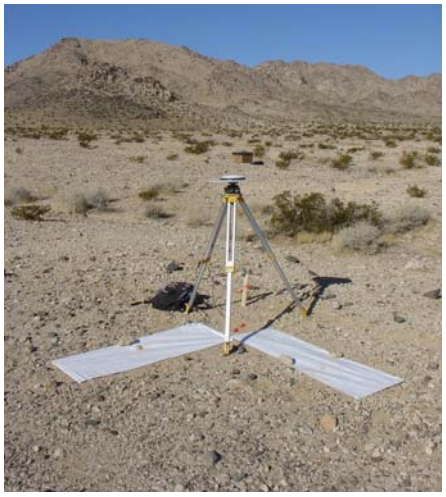

Example Victorville control point

On February 4, 2006, calibration flights were conducted. A laser pulse rate of 40 kHz was selected as most appropriate to meet overall point density targets. Orthophoto flights began on January 24, 2006 and lidar acquisition flights began on February 3, 2006.

**Figure 3-6**
**Victorville Test Craters**

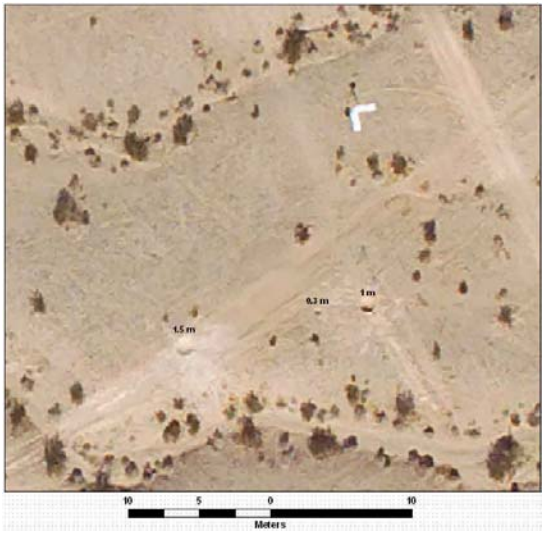


Sample test craters

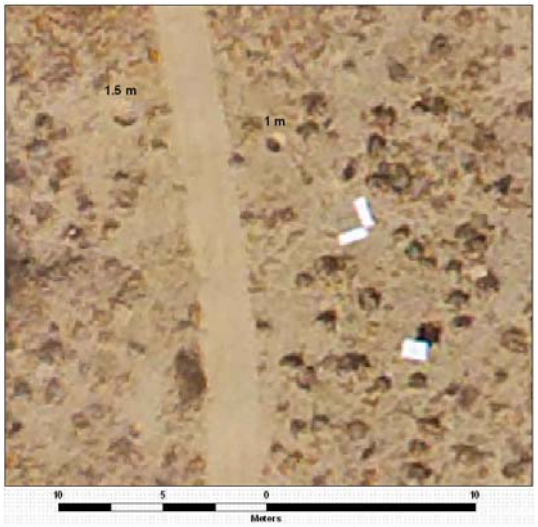


Sample test craters and vertical control structure

## 3.5 TESTING AND EVALUATION PLAN AND PROCEDURES

### 3.5.1 Demonstration Set-Up and Start-Up

At both sites, TRSI conducted flight line planning for the lidar/orthophoto and lidar only flights in the weeks prior to mobilization. Flight lines were planned to ensure complete site coverage, minimize the number of turns, and achieve planned overlap. At the Kirtland site, flight lines were planned to minimize interactions between data collection and air traffic at the Double Eagle Airport. Digital imagery was planned for acquisition at periods of low sun angle at both sites. Previous testing had shown that the shadows created by low sun angle were useful in detecting shallow features.

At each site, the lidar and orthophoto sensor system was installed into a Bell 206B helicopter owned by a local helicopter vendor (Figure 3-7). Renting helicopters (and pilots) using local vendors is a standard industry practice which allows the lidar vendor to ship only the sensor package rather than the aircraft. The use of local helicopter vendors also allows for the use of local pilots who have better knowledge of local weather patterns and flight clearance requirements.

**Figure 3-7**
**Lidar Equipment Setup**

Equipment installation

Sensor pod mounted below helicopter, control console visible through window

### 3.5.2 Period of Operation and Area Characterized

Data collection flights were begun once mobilization, sensor installation, and calibration flights were complete. The period for data collection included an additional day to allow for re-acquisition of any missed or erroneous areas discovered during daily quality assurance/quality control (QA/QC) review. Data collection periods were as shown on Table 3-1.

**Table 3-1**
**Data Collection Periods**

| Period | Kirtland | Victorville |
|---|---|---|
| Preflight planning | July 2005 | January 2006 |
| Mobilization | August 8, 2005 | February 7, 2006 |
| Calibration flights | August 8, 2005 | February 8, 2006 |
| Data collection | August 9-11, 2005 | January 24-25, 2006<br>February 3-4, 2006 |
| Demobilization | August 1, 2005 | February 5, 2006 |

At Kirtland, the area characterized was 1,914 hectares or 5,000 acres. At Victorville the area was 2,282 hectares or 5,640 acres.

### 3.5.3 Demobilization

Demobilization of the lidar and orthophoto equipment consisted of demounting the sensor system from the helicopter, packing and shipping. Demobilization required approximately a half day for each site.

## 3.6 SELECTION OF ANALYTICAL/TESTING METHODS

Analysis of lidar data is performed in two steps: conversion of sensor output to spatially correct lidar points, and then conversion of these points to useable GIS products such as surface models. Lidar data was processed into point files using a suite of software, including TerraSolid and custom algorithms written in this software by TRSI. TerraSolid is an industry standard software package for processing lidar data.

Creation of GIS products and their analysis were accomplished using ESRI's ArcGIS software suite. This package was chosen for two reasons. First, ArcGIS was the only standard CAD or GIS product reviewed that would successfully handle the large number of lidar points collected. Second, ArcGIS is the GIS package most widely used by US government agencies and private contractors. As such, it is appropriate to develop analysis methods and resulting products that can be duplicated by typical federal facilities managers.

Orthophoto data was analyzed in two steps: creation of a single orthorectified image from the large number of individual digital images collected, followed by visual examination of the image to locate potential MRS and munitions-related features. Processing of the digital imagery to create the orthophoto mosaic was accomplished using software from TerraSolid and PCI. This software is the industry standard.

## 3.7 RESULTS

### 3.7.1 Data Collection

At the Kirtland site, data collection flights took place on August 9, 10, and 11, 2005 with a total of 177 flight lines collected, totaling 555 km. Lidar data was collected at three altitudes: 900 meters, 450 meters, and 300 meters (Figure 3-8). Two sets of flight lines were flown at 300 meters. For the north portion of the project area the 300 meter flight lines were flown perpendicular to each other, for the south portion they were flown parallel. Orthophoto data was collected concurrently with lidar during the 900 meter and 450 meter flights.

**Figure 3-8**
**Kirtland Sample Flight Lines**

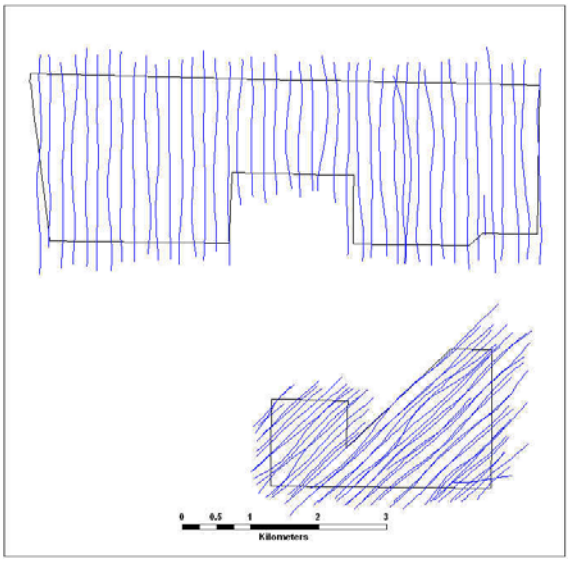


Kirtland flight lines, 300 m lidar flight 2

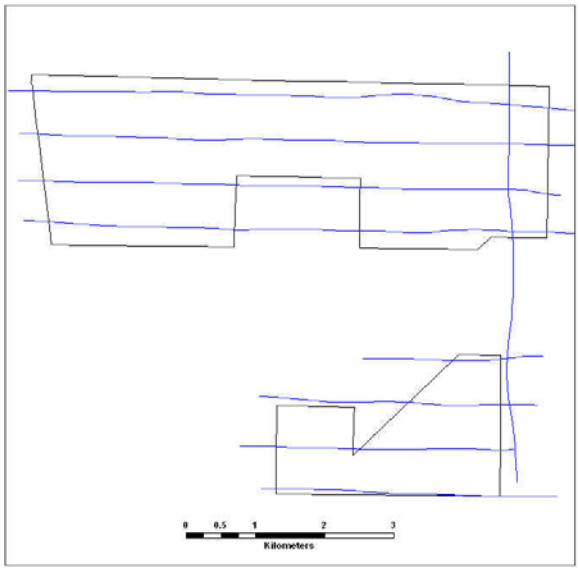


Kirtland flight lines, 900 m lidar and 20 cm orthophotos

Data was inspected each evening for GPS positional accuracy, completeness of lidar data coverage and imagery data coverage. During the final afternoon of data collection, flight lines that did not meet specifications were re-flown.

At the Victorville site, orthophoto data collection flights took place on January 24 and 25, 2006 and lidar data collection flights took place on February 3 and 4, 2006. A total of 45 flight lines were collected, totaling 601 km. Lidar data was collected at two altitudes: 450 meters and 300 meters (Figure 3-9). The two flights were flown perpendicular to each other. As at the Kirtland site, data was inspected each evening for accuracy and completeness, and data gaps were filled by additional flights prior to demobilization.

**Figure 3-9**
**Victorville Sample Flight Lines and Example Image**

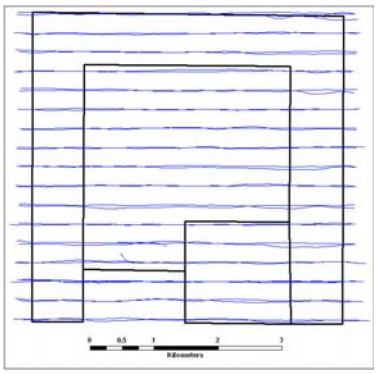

Victorville flight lines, 300 m lidar flight

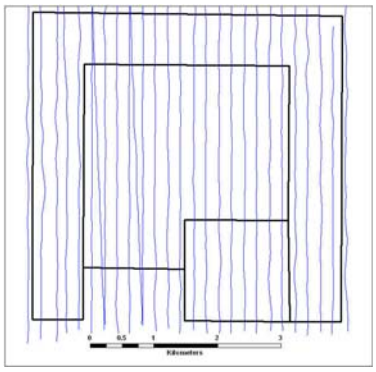

Victorville flight lines, 450 - m lidar and 10 cm orthophotos

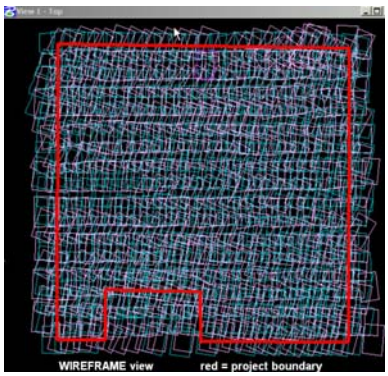


Example image from software used to check for complete coverage by digital imagery, 450 m flight

### 3.7.2 Safety Issues

At the Kirtland site, an important safety issue was the high level of air traffic at the Double Eagle Airport. This airport experiences more than 100,000 take-offs per year, and is located immediately adjacent to the study site between the north and south blocks. In response to the high level of air traffic, a second pilot was hired to be a spotter during data collection flights. This extra weight led to more frequent refueling and longer data collection work days. The air traffic situation also prevented the acquisition of perpendicular lidar flight lines for the south block, which would have required turning directly over the runway.

### 3.7.3 Data Processing Steps

TSRI processed the sensor output to create lidar points. Following return of the data to the office, calibration factors determined in the field were checked, fine-tuned, and applied to laser range, GPS, and IMU data to produce x,y,z values for each point. Lidar points were then transformed into the delivery datum and projection for each site, and coded to indicate returns from ground vs. non-ground surfaces. Lidar points were exported as text files for delivery to URS. Lidar data from each lidar flight was processed and delivered separately in order to allow for separate analysis of data from each flight altitude.

TSRI also processed digital images. The procedure included mosaicing the individual digital images collected during flight, transforming the consolidated image to the delivery datum and projection, orthorectification using the lidar data, color balancing, and trimming to the delivery tiles. For the Kirtland site, two sets of orthomosaics were created, one at 10 cm pixel size and one at 20 cm pixel size. For the Victorville site, a single set of orthophotos was created at 10 cm pixel size.

URS converted the random lidar point data to GIS products using the following steps:

- The lidar points were converted to ArcInfo point shape file format, with the horizontal locations determined by the northing and easting values in the lidar point file, and the elevation value, intensity value, and the code for ground or non-ground return retained as attributes.

- Point shape files were converted to Triangulated Irregular Network (TIN) files. A TIN is an elevation-based surface model where each point forms a vertex in a network of linked triangles. TINs were created from the lidar points coded as ground returns, using ArcInfo's TIN creation functions. A TIN was created for each lidar flight separately. For the Kirtland data, an additional TIN was created for the combined 300 meter flights, the combined 450 meter and 900 meter flights, and the points from all four flights. For the Victorville data, a TIN was created containing point from both flights. TINs were also created in selected areas using both ground and non-ground returns, in order to derive vegetation heights and to allow for QA/QC review of point classification as ground or non-ground returns.

- Digital elevation models (DEMs) were created from the TINs. A DEM is a regularly spaced, gridded array of elevation values. DEMs were created using the each of the TIN files as inputs. DEMs were created in the ArcInfo GRID file format, which allows for additional analysis that cannot be performed directly on the TIN file. All DEMs were created using 0.32 meter (1 foot) grid cell sizes. This value was chosen as the smallest cell size that would be supported by the lidar data densities acquired.

Automated GIS processing and analysis was used for many of the process steps.

Once the initial GIS products were created, the lidar data were examined to detect missing data, spatial discrepancies, or artifacts in the surface that would indicate improper calibration or other problems. Further data quality review, including review for spatial accuracy, was performed based on the parameters given in Appendix C of the Technology Demonstration Plan. All data met data quality specifications. Detailed results are given in Appendix A, Lidar and Orthophoto Positional Accuracy Results.

Following creation of initial GIS products and initial QA/QC review, analysis of the lidar and orthophoto data was conducted by URS:

- Hillshades were created for each of the DEMs. Hillshades are three-dimensional depictions of the surface with shadows formed by a simulated light source placed above the surface at an altitude and azimuth chosen by the operator. The default settings for hillshades in ArcGIS Spatial Analyst were used, then varied as needed during the analysis. Hillshades were saved in ArcInfo GRID format.

- Each lidar hillshade and orthophoto data set was visually inspected for potential MRS. Potential MRS were identified and drawn as ArcInfo line or polygon shape files for each data set.

- Each data set was visually inspected for potential munitions-related features. Potential features were drawn as ArcInfo line or polygon shape files for each data set. Potential features were classified according to naming standards provided by ESTCP.

- A slope model was created for each demonstration site. The process used the default setting for the ArcGIS SLOPE GRID command.

- Models of elevation above and below an average ground surface were created for each lidar data set. The process used the ArcInfo Focal Mean function.

### 3.7.4 Detection and Delineation of Munitions Response Sites

At the Kirtland site, all four of the MRS described in the Kirtland CSM were detected using lidar, and three of the four were detected using orthophotos. In addition, both technologies revealed additional potential sites of interest.

Table 3-2 presents Kirtland MRS detection results for each of the lidar and orthophoto data sets.

**Table 3-2**
**MRS Detection – Kirtland**

| | MRS from CSM | | | | Additional Sites of Interest |
|---|---|---|---|---|---|
| | N2 | N3 | NDIA | SORT | |
| **Orthophotos** | | | | | |
| 20 cm | Y | Y | Y | N | 1 |
| 10 cm | Y | Y | Y | N | 1 |
| **Individual lidar flights** | | | | | |
| 900 m | Y | Y | Y | Y | 6 |
| 450 m | Y | Y | Y | Y | 7 |
| 300 m flight 1 | Y | Y | Y | Y | 7 |
| 300 m flight 2 | Y | Y | Y | Y | 7 |
| **Combined lidar flights** | | | | | |
| 450 and 900 m | Y | Y | N | Y | 6 |
| Both 300 m | Y | Y | Y | Y | 5 |
| All lidar | Y | Y | N | Y | 5 |

As lidar data from different flights was combined, the number of additional potential MRS identified and the overall area mapped as MRS began to drop. This phenomenon is described more fully in Appendix B, Combining Lidar Data from Multiple Flights.

At the Victorville site, both MRS described in the initial CSM were detected, and were visible in both lidar data sets and the single orthophoto data set. No additional sites of interest were detected at Victorville using these technologies.

The following sections review data for each MRS listed in the Kirtland CSM in more detail.

### 3.7.5 Kirtland – Target N3 Results

Target N3 is described in the CSM as a 1,000-foot diameter bull's-eye target used for 100-pound practice bombs and scrap storage. In addition to the bull's-eye rings, three potential ancillary targets and one additional area of interest were identified that were not listed in the CSM: a ship target east of the bull's-eye, a simulated airfield target to the south, a diamond-shaped potential target to the west, and a small rectangular feature to the north. The bull's-eye rings consist of berms between 5 and 10 cm high and a mound at the center point approximately 80 cm high. The ship target consists of berms ranging from 60 cm in height on the north end to essentially flush with the ground surface on the south end. The diamond-shaped potential target consists of trenches from 20 to 70 cm deep in the corners.

**Table 3-3**
**Target N3 Detection Results**

| | Rings | Ship | Airstrip | Diamond | Small Rectangle | Total Area of MRS ($m^2$) |
|---|---|---|---|---|---|---|
| **Orthophotos** | | | | | | |
| 10 cm | 5 | N | N | Y | N | 195,258 |
| 20 cm | 5 | N | N | Y | N | 195,258 |
| **Individual lidar** | | | | | | |
| 900 m | 4 | Y | Y | Y | N | 992,977 |
| 450 m | 5 | Y | Y | Y | N | 1,226,982 |
| 300 m 1 | 5 | Y | Y | Y | Y | 1,226,982 |
| 300 m 2 | 5 | Y | Y | Y | Y | 1,226,982 |
| **Combined lidar** | | | | | | |
| 450 and 900 m | 5 | Y | Y | Y | N | 1,226,982 |
| Both 300 m | 5 | Y | | | | 992,977 |
| All lidar | 5 | Y | Y | Y | Y | 992,977 |

Figure 3-10 shows the Target N3 target elements detected.

**Figure 3-10**
**Target N3 Elements**

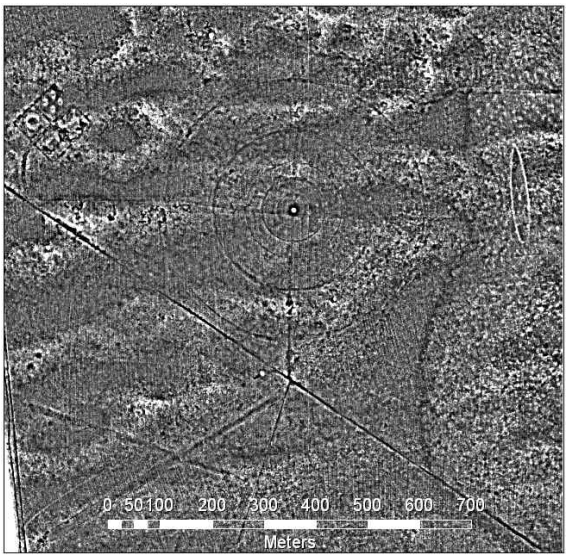


Target N3, 300 m lidar, showing target bull's-eye rings, ship target (east), diamond-shaped potential target (west), and simulated air strip (south).

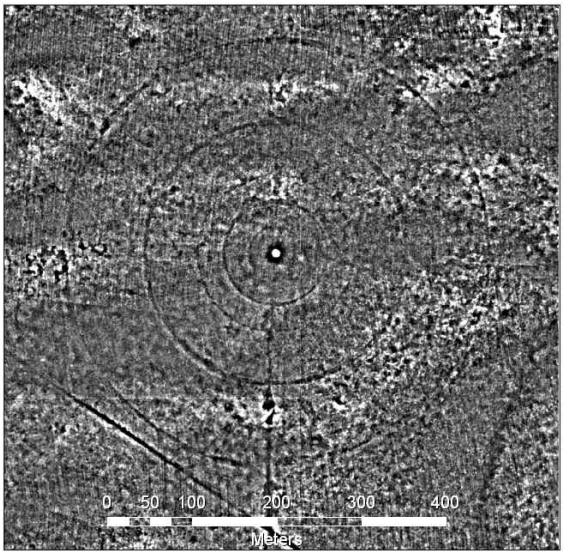


Target N3 bull's-eye rings, 450 m lidar displayed as elevations above an average ground surface.

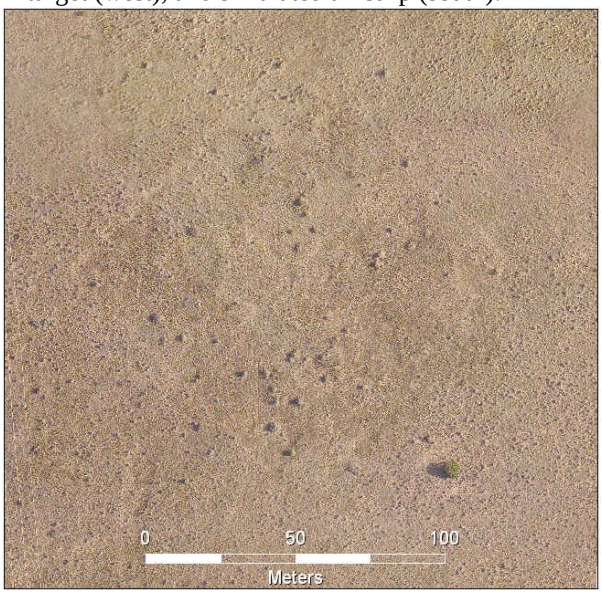


Diamond-shaped potential target west of N3 bull's-eye, 20 cm pixel orthophoto. Feature is approximately 100 m on each side.

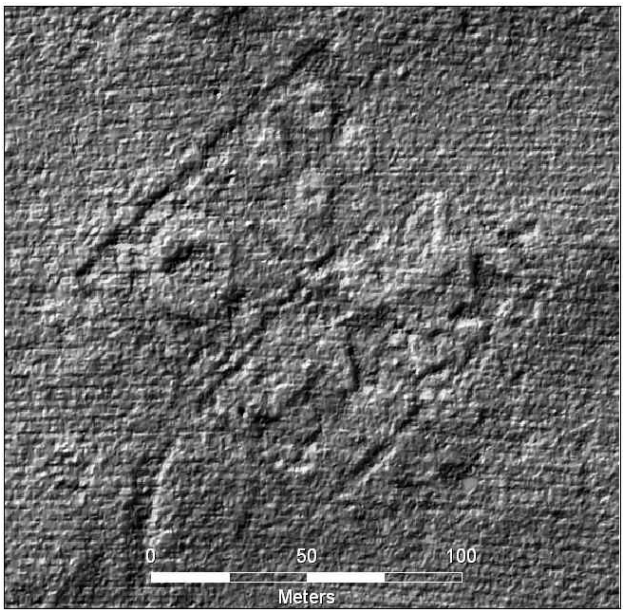


Diamond-shaped potential target west of N3 bull's-eye, 300 m lidar. Feature is similar in all lidar data sets.

**Figure 3-10 (continued)**
**Target N3 Elements**

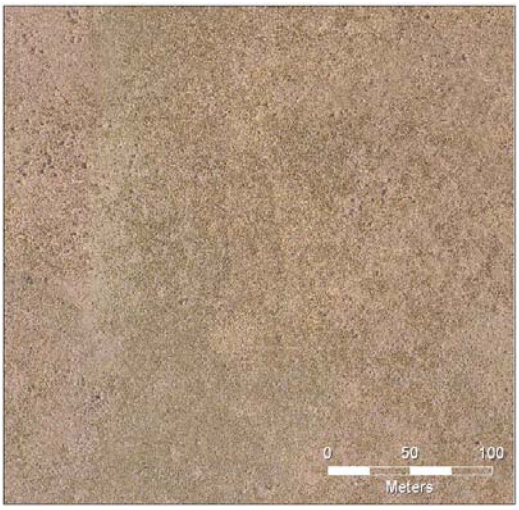


Ship target east of N3, 10 cm pixel orthophoto.

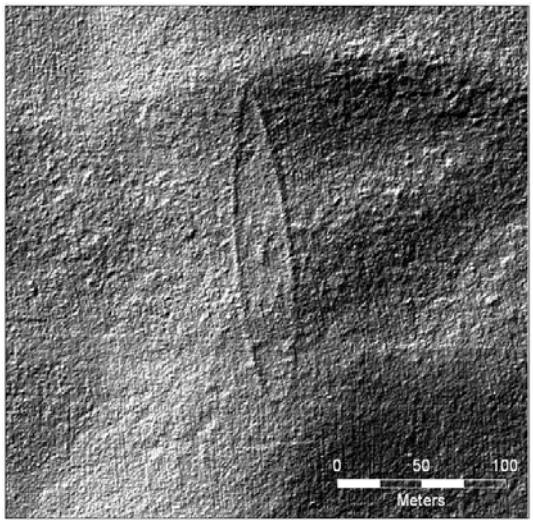


Ship target east of N3 shown in 300 m lidar surface combined with a 300 m lidar subtracted grid to enhance the image.

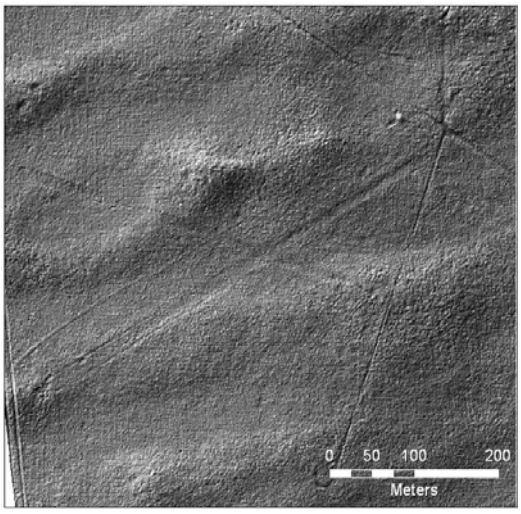


Airstrip target south of N3 bull's-eye.

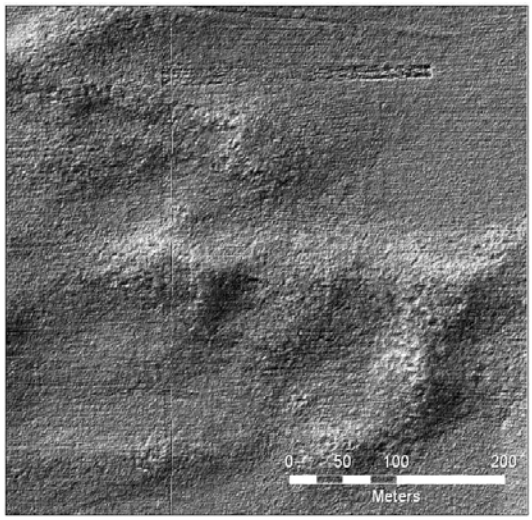


Small rectangular area of interest north of N3 bull's-eye.

### 3.7.6 Kirtland – Target N2 Results

Target N2 is described in the CSM as a bull's-eye target used for 100-pound practice bombs. The bull's-eye rings were visible using lidar data; there were few to no visible craters. Three rings were visible using the orthophotos at both pixel sizes, and four were visible in the lidar

data, regardless of data density. Because of the different number of rings visible, the total area of this MRS from the orthophotos was 26,234 $m^2$, while the total area from the lidar data was 74,753 $m^2$. The bull's-eye rings consist of berms between 5 and 10 cm high. Figure 3-11 shows the Target N2 target elements detected.

**Figure 3-11**
**Target N2 Orthophoto and Lidar**

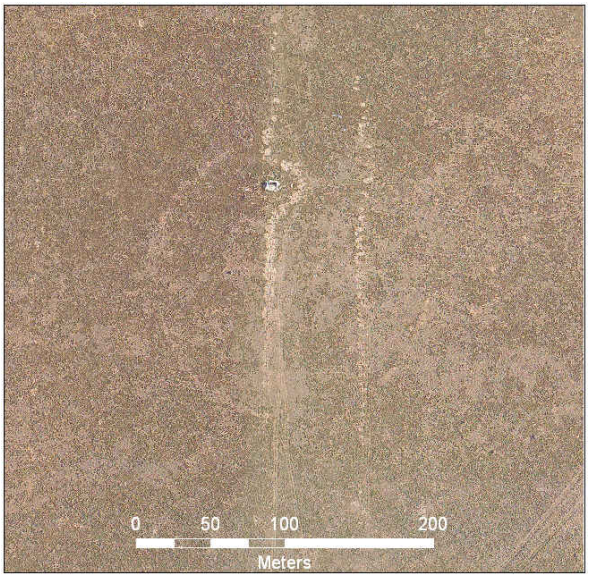

Target N2 bull's-eye, 20 cm pixel orthophoto

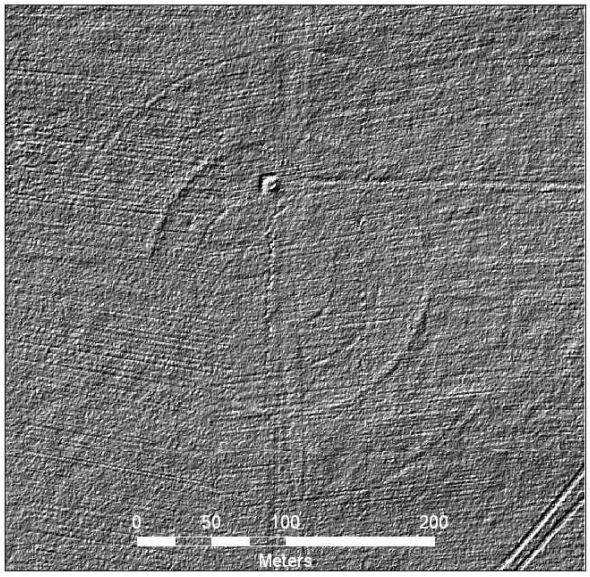

Target N2 bull's-eye, 300 m lidar

### 3.7.7 Kirtland – Target NDIA Results

The NDIA is described in the CSM as a 1,000 foot diameter HE bull's-eye target. Target cross-hairs and a single bull's-eye ring were visible in the orthophotos at both pixel sizes; neither was visible in the lidar data at any data density. A large number of probable craters was visible in the lidar data, with the number counted increasing with data density, then decreasing as data from the individual flights was combined. These craters were used to define the boundary of the MRS. Craters were not visible in the orthophoto data. Table 3-4 shows the features detected with each data set. Potential craters ranged from 1 to 3 meters in diameter and from 10 to 20 cm in depth.

**Table 3-4**
**Target NDIA Detection Results**

| | Probable Craters | Rings | Cross-hairs | Total Area ($m^2$) |
|---|---|---|---|---|
| **Orthophotos** | | | | |
| 10 cm | 0 | 1 | 2 | 78,251 |
| 20 cm | 0 | 1 | 2 | 78,251 |
| **Individual lidar** | | | | |
| 900 m | 25 | 0 | 0 | 182,356 |
| 450 m | 34 | 0 | 0 | 182,356 |
| 300 m 1 | 44 | 0 | 0 | 182,356 |
| 300 m 2 | 39 | 0 | 0 | 182,356 |
| **Combined lidar** | | | | |
| 450 and 900 m | 34 | 0 | 0 | not found |
| Both 300 m | 29 | 0 | 0 | 182,356 |
| All lidar | 33 | 0 | 0 | not found |

Figure 3-12 illustrates the complementary ability of lidar and orthophotos to define this target area, with the orthophoto image showing the cross-hairs and target rings, and the lidar data showing the probable craters.

**Figure 3-12**
**Target NDIA Orthophoto and Lidar**

Target NDIA 20 cm orthophoto showing target crosshairs and bull's-eye ring. Craters could not be seen in the orthophotos.

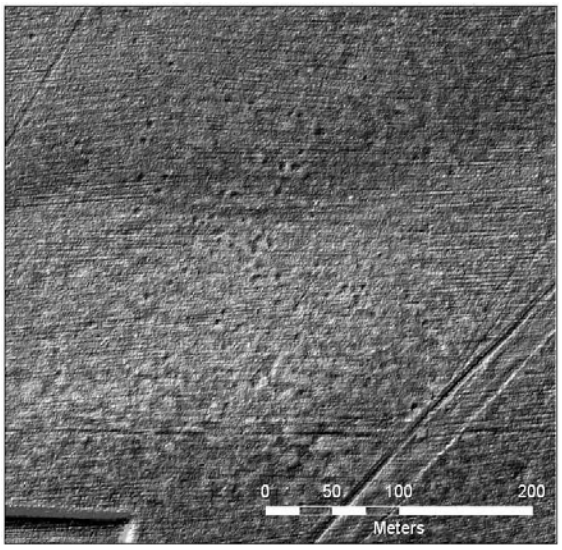


Target NDIA 300 m lidar showing craters. Cross-hairs and bull's-eye ring could not be seen using lidar.

### 3.7.8 Kirtland – Target SORT Results

The SORT is described in the CSM as a suspected target whose location is given as "somewhere northwest of the airport." The target was identified as a 23-acre rectangle subdivided into cells simulating an oil tank farm. This target was located using lidar data at all densities, but was not visible in either of the orthophoto sets (Figure 3-13). The target cells consist of berms from 0 to 20 cm in height.

**Figure 3-13**
**Target SORT Orthophoto**

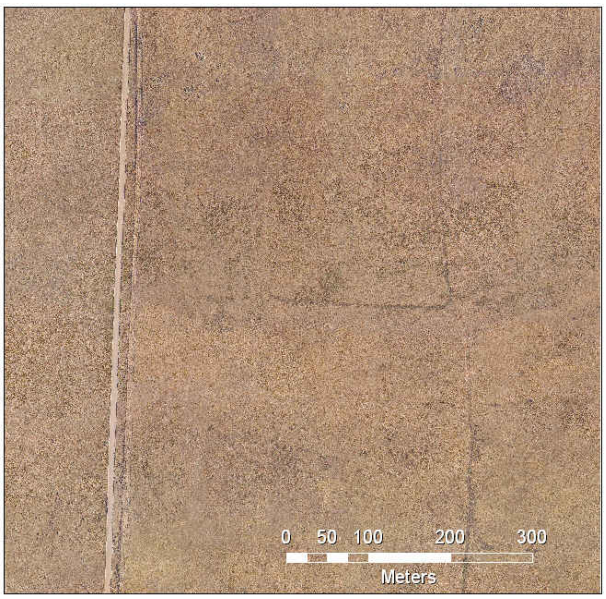


Target SORT, 10 cm pixel orthophotos. The target was not visible in either orthophoto data set.

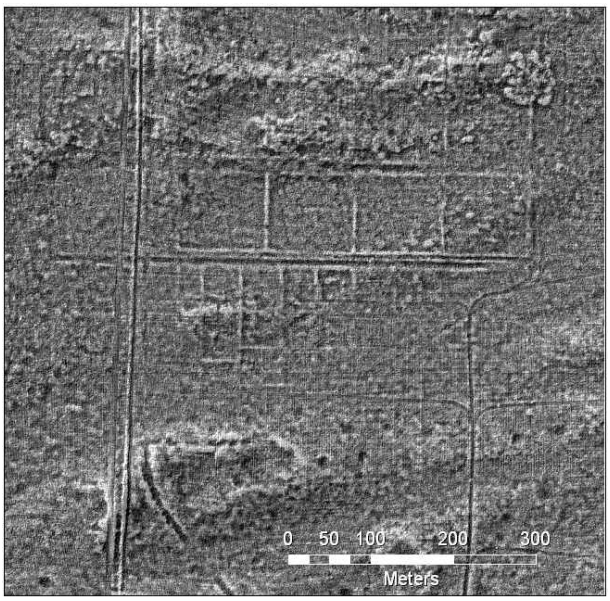


Target SORT, 300 m lidar. The target was visible in lidar data at all densities collected.

### 3.7.9 Kirtland – Other Sites of Interest

At the Kirtland site, 15 additional sites of interest were detected using the lidar data, including seven in the north portion of the site and eight in the south portion (Figure 3-14). One area in the south portion consisted of a previously unknown potential target bull's-eye; the remainder consisted of small groupings of potential craters and the small rectangular feature north of Target N3. All of these potential MRS were detected using lidar data; none was visible in the orthophotos. The potential craters are generally larger and more irregular than would be expected from any of the munitions mentioned in the initial CSM, and their sizes are irregular. It is possible that these features may be related to burial or other munitions management activities; however, the lidar data do not indicate a high confidence that these areas are related to munitions use. Rather, these are areas that warrant further investigation.

**Figure 3-14**
**Sample Additional Sites of Interest**

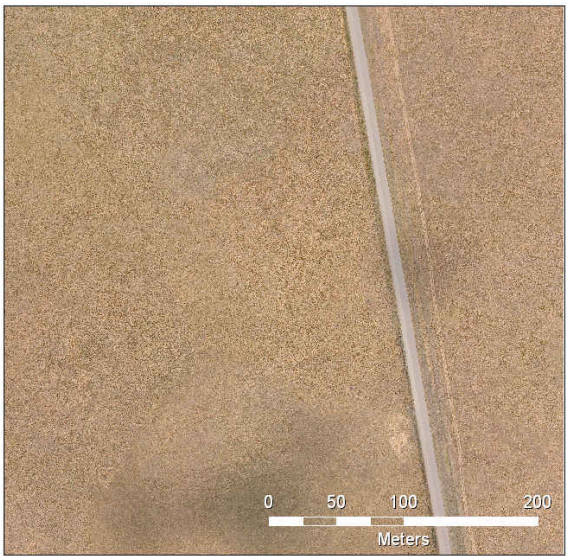


Previously unknown potential target bull's-eye, 10 cm pixel orthophoto. Potential target was not visible.

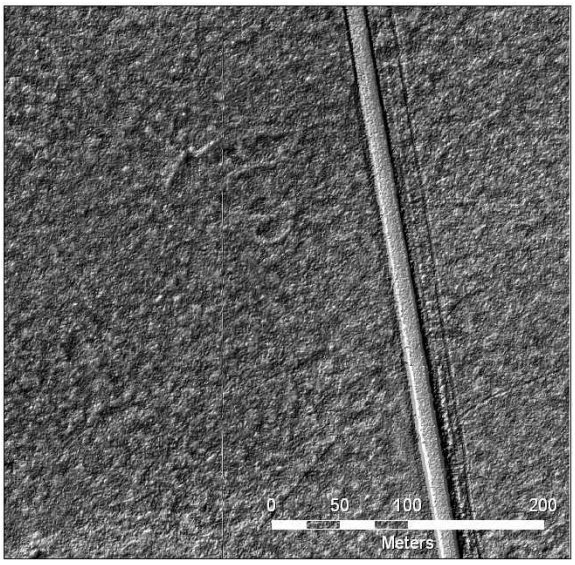


Previously unknown potential target bull's-eye, south portion of site, 300 m lidar. Identified in CSM as KPBR-AOI-4.

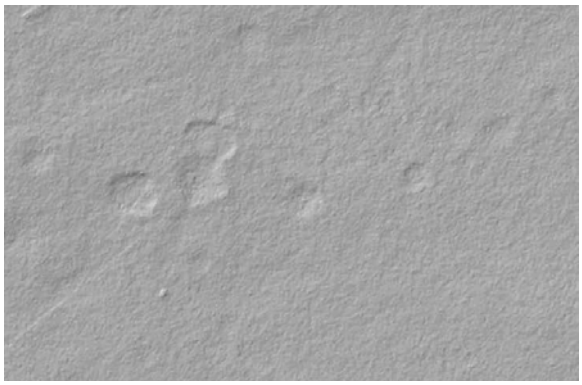

Craters forming potential MRS, 450 m lidar. This area is identified in the CSM as KPBR-AOI-10.

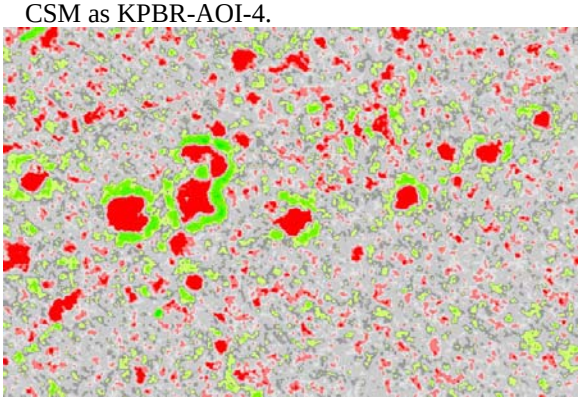

Craters forming potential MRS, elevations coded as below (red) and above (green) the ground surface.

### 3.7.10 Victorville – Target DBT Y Results

Target DBT Y is described in the CSM as the bed of Means Dry Lake, an area of approximately 345 acres. This area was clearly visible using both lidar and orthophotos, and the delineated boundary of the dry lake bed was not different between the lidar and orthophotos, nor for any of the lidar data densities tested (Figure 3-15).

**Figure 3-15**
**Target DBT Y Orthophoto and Lidar**

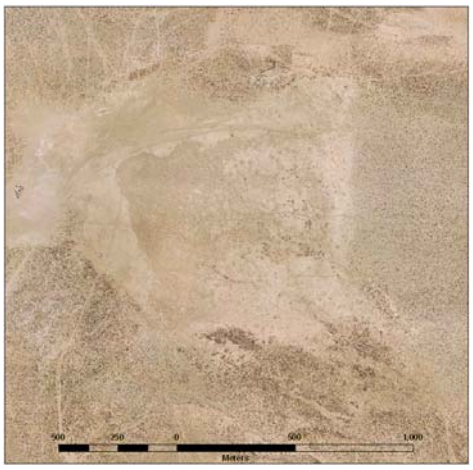


Target DBT Y, orthophoto

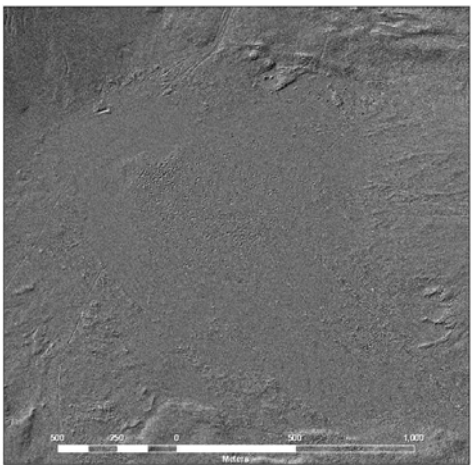


Target DBT Y, combined lidar

### 3.7.11 Victorville – Target PBR 15 Results

Target PBR 15 is described in the CSM as a bull's-eye target used for precision bombing practice. The target was clearly visible in the orthophotos. Initially, the target was difficult to detect using lidar, since the bull's-eye rings are formed from asphalt laid flat on the relatively flat ground surface. The target thus has very little vertical relief to be detected by lidar. However, an image of the area created using the lidar intensity values showed the target clearly (Figure 3-16). Target ring dimensions were 60 m (197 feet) for the smallest ring, 120 m (394 feet) for the middle ring, and 190 m (623 feet) for the outer ring.

**Figure 3-16**
**Target PBR 15 Orthophotos, Lider Surface Model and Lidar Intensity Image**

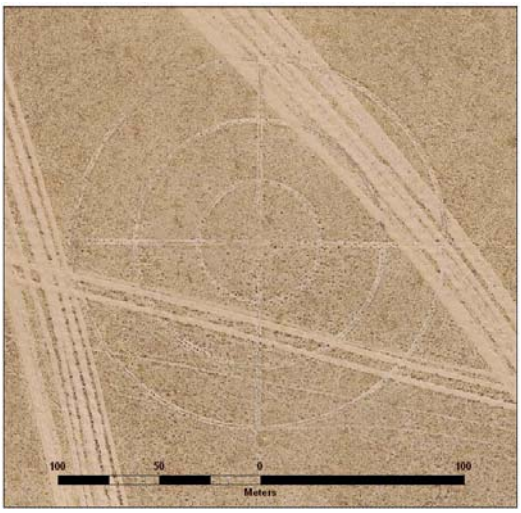

Target PBR 15, orthophoto.

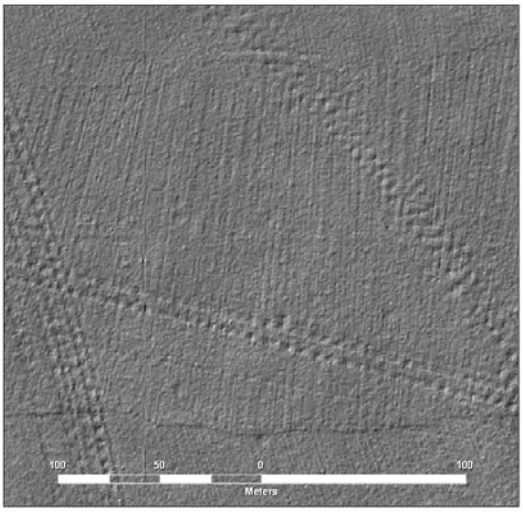

Target PBR 15, 300 m lidar.

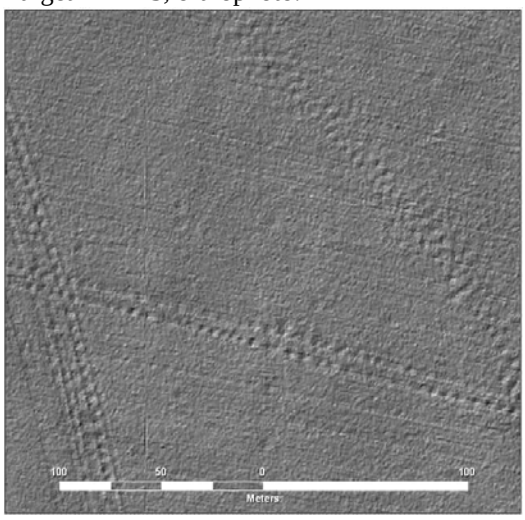

Target PBR 15, 450 m lidar.

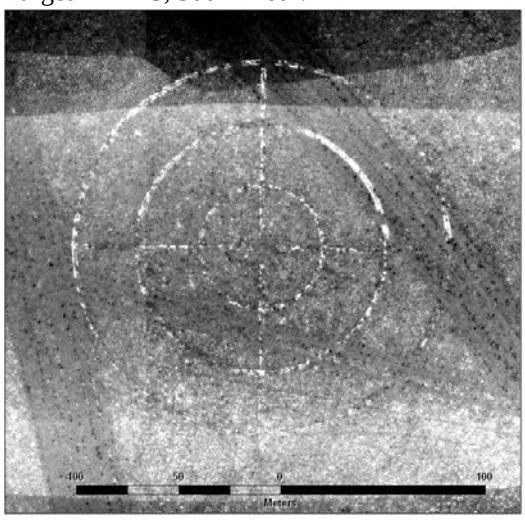

Target PBR 15, lidar intensity.

### 3.7.12 Detection of Potential Munitions-Related Ground Features

The Kirtland site contained just over one hundred small features that were potentially related to munitions use, mostly potential craters. The site also contained numerous linear features, mostly jeep trails and other vehicle tracks. Potential features were visually identified from the lidar hillshades and the orthophotos. The extremely shallow nature of the potential craters near Target NDIA (10 – 20 cm) made many of them difficult to distinguish with confidence from the natural ground surface. Consequently, the numbers given for objects detected should be understood as a comparison of the various data sets rather than a conclusive number of MEC-related features.

The number of features detected at the Kirtland site also varied depending on the method used to display the lidar data (Figure 3-17), particularly for the weathered craters near Target NDIA. This suggests that these potential craters were near the detection limit of this technology.

**Figure 3-17**
**Kirtland Target NDIA Potential Crater Detection**

Target NDIA, cross hairs and target center, 10 cm pixel orthophoto.

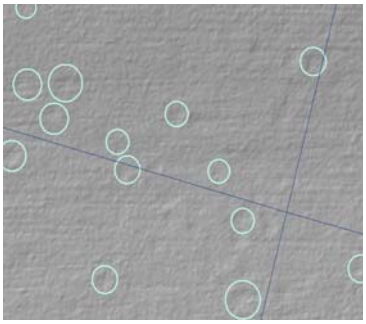

Target NDIA, craters identified from lidar hillshade alone.

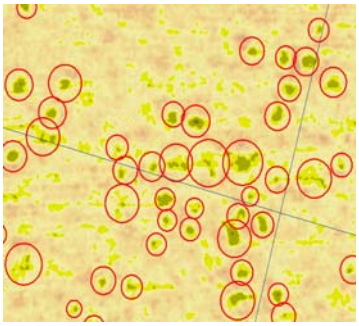

Target NDIA, craters identified from lidar surface model color-coded to show depths of depressions.

At Victorville, potential craters in Means Dry Lake were much larger than at any of the Kirtland targets, ranging from 5 to 8 m in diameter and up to 1 m deep. Unlike the smaller craters at Kirtland, the craters at Victorville were clearly visible in the orthophotos (Figure 3-18). A significant number of potential craters were located outside and northwest of the lake boundary.

**Figure 3-18**
**Victorville Target DBT/Craters, Orthophotos and Lidar**

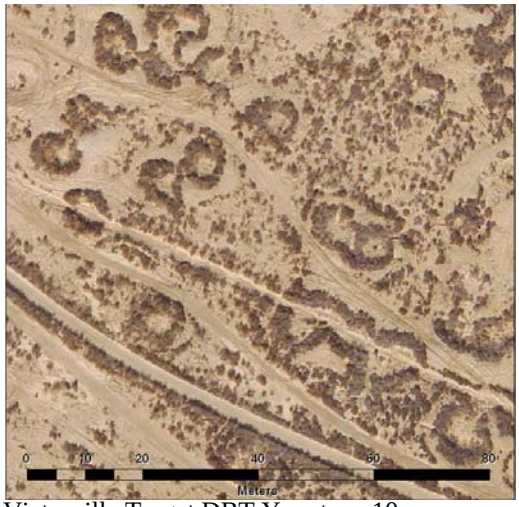


Victorville Target DBT Y craters, 10 cm orthophotos

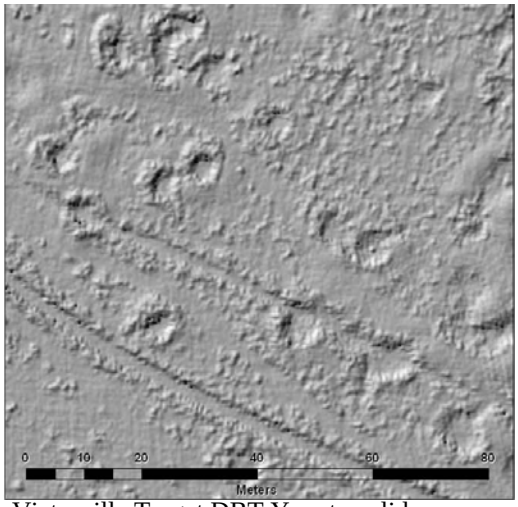


Victorville Target DBT Y craters, lidar surface model including vegetation point

**Figure 3-18**
**Victorville Target DBT/Craters, Orthophotos and Lidar (continued)**

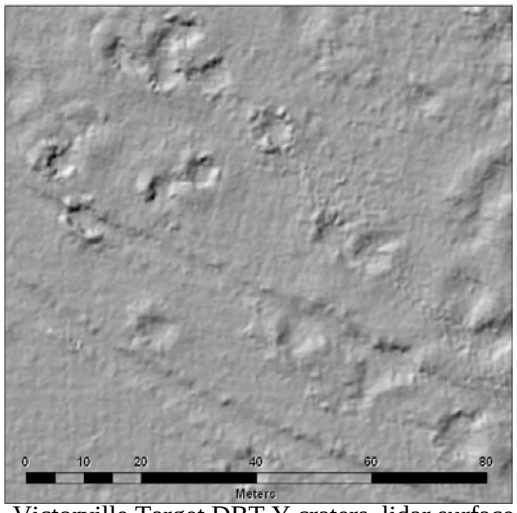


Victorville Target DBT Y craters, lidar surface model, ground points only

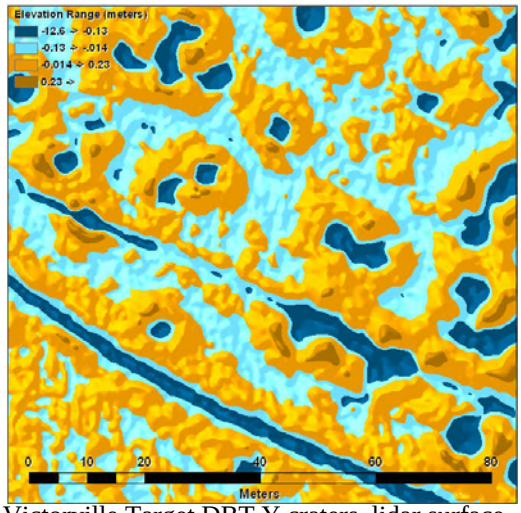


Victorville Target DBT Y craters, lidar surface model, ground points only, color-coded to show feature heights and depths.

The potential crater locations outside of the dry lake bed were used to modify the location of the target area boundary. Following this modification, the size of the potential MRS increased from the original 345 acres to 641 acres (Figure 3-19).

**Figure 3-19**
**Victorville Target DBT Y - MRS Boundaries**

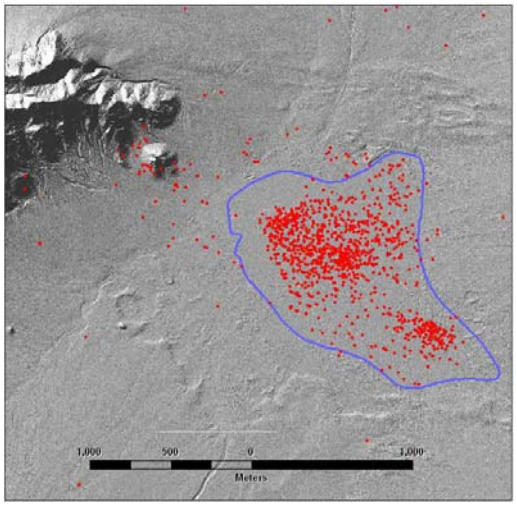


Victorville Target DBT Y, MRS boundary from CSM.

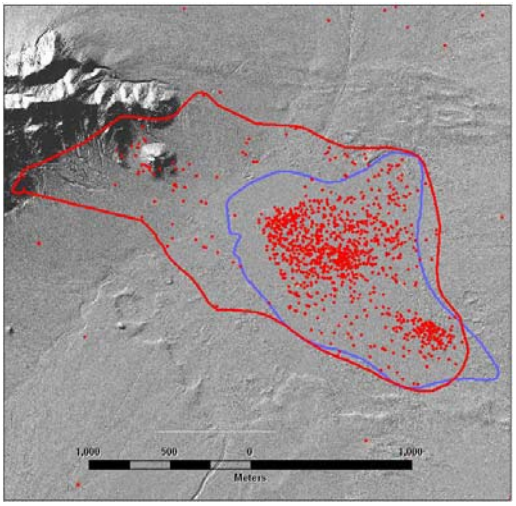


Victorville Target DBT Y, MRS boundary following modification using feature locations.

No craters were detected at Target PBR 15. This is consistent with its reported use as a practice bombing target. There were no other potential munitions-related features at the target, other than the asphalt target rings themselves.

### 3.7.13 Data Density Effects - General Results

The test crater area at the Kirtland site was used to examine the general effects of lidar and orthophoto data density. Orthophoto data density was examined first, based on the size of the image pixels. Figure 3-20 shows the test crater area in the 10-cm and 20-cm pixel data sets. The 10 cm orthophotos and the known dimensions of the test craters were used to create the "best" locations for the test craters; these were then superimposed on the 20 cm photo.

**Figure 3-20**
**Kirtland Test Craters, Orthophotos**

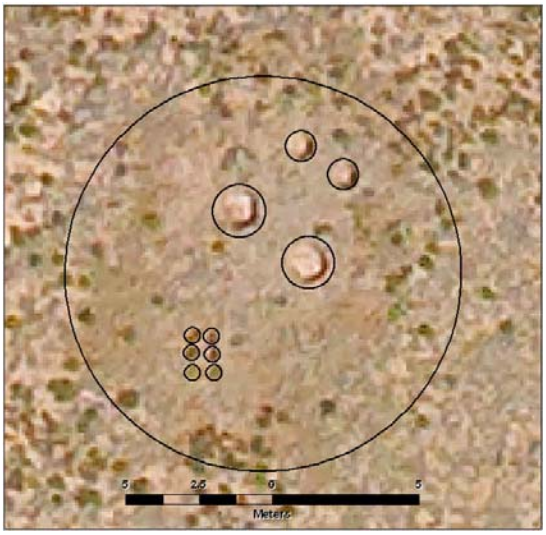

10 cm orthophoto with "best" crater locations.

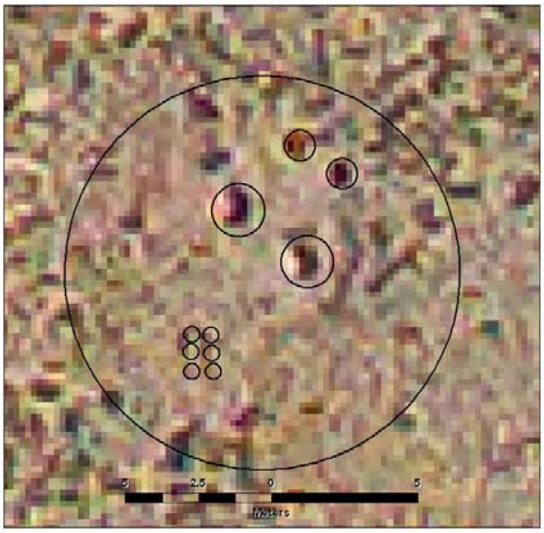

20 cm orthophoto with "best" crater locations.

These images illustrate the substantial difference in clarity between the 10 cm and 20 cm pixel orthophotos. All 10 test craters are visible in the 10 cm orthophoto, although the 0.32 m craters are distinguishable from surrounding objects primarily through their regular pattern. The 1.5 and 1.0 m craters are visible in the 20 cm pixel orthophoto; however, neither can be clearly distinguished from the surrounding ground features. This comparison led to the decision to acquire only 10 cm pixel orthophotos at the Victorville site.

Lidar data density was examined based on the average number of points per square meter. Lidar data was obtained at the overall data densities shown in Table 3-5.

**Table 3-5**
**Achieved Lidar Data Densities**

| Demonstration Site | Flight | Point density (pts/m$^2$) |
|---|---|---|
| **Kirtland** | 900 m North Block | 1.4 |
| | 900 m South Block | 1.6 |
| | 450 m north block | 5.2 |
| | 450 m south block | 4.1 |
| | 300 m east-west north block | 5.2 |
| | 300 m north-south north block | 6.5 |
| | 300 m flight 1 south block | 5.9 |
| | 300 m flight 2 south block | 6.1 |
| **Victorville** | 450 m flight | 4.8 |
| | 300 m flight | 6.4 |
| | Combined 300 and 450 m flights | 11.2 |

These overall lidar data densities are a general representation based on statistics for the site as a whole. In fact, lidar data density varies considerably over the ground surface, a complex phenomenon that is discussed in Appendix C.

Figure 3-21 shows hillshades of the four lidar data sets at the Kirtland test craters, using the ground returns only. The locations of the test craters are taken from the 10 cm orthophoto data and superimposed on the lidar images.

**Figure 3-21**
**Kirtland Test Craters, Lidar Surface Models**

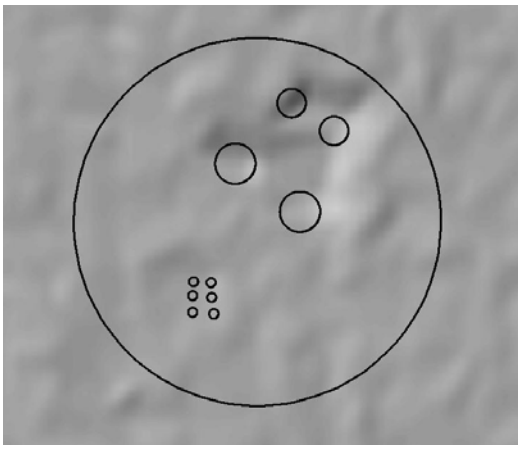

Kirtland test craters, 900 m (1.6 pts/ m$^2$) lidar hillshade, ground points only.

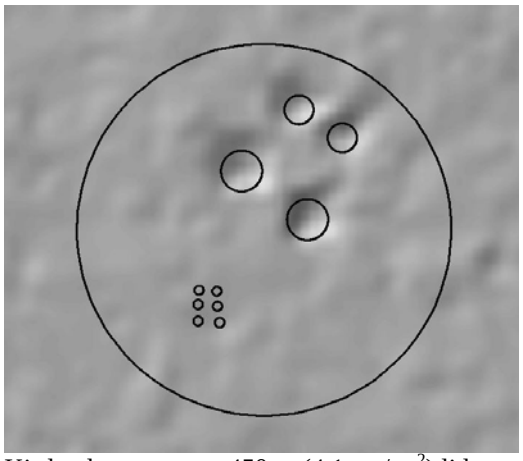

Kirtland test craters, 450 m (4.1 pts/ m$^2$) lidar hillshade, ground points only

**Figure 3-21**
**Kirtland Test Craters, Lidar Surface Models (continued)**

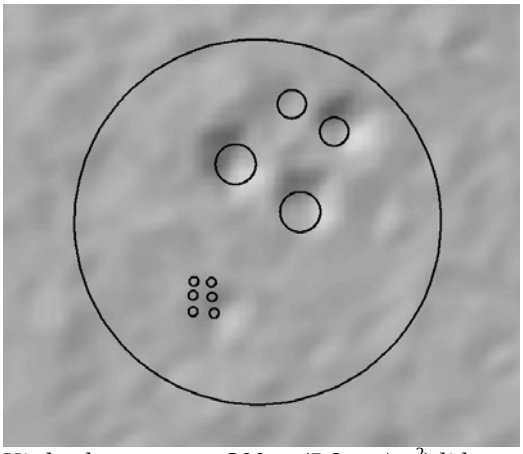

Kirtland test craters, 300 m (5.9 pts/ $m^2$) lidar flight 1 hillshade, ground points only.

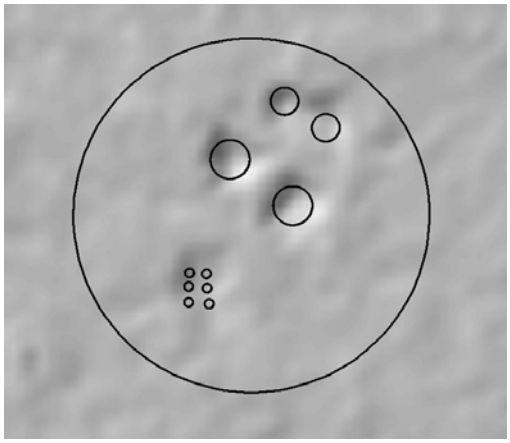

Kirtland test craters, 300 m (6.1 pts/ $m^2$) lidar flight 2 hillshade, ground points only.

These images show that craters are more clearly defined as the density of the lidar points increases. In the 900 m lidar data, the crater area appears as a single depression and the individual craters cannot be detected. In the 450 m lidar data, the 1.5 and 1.0 meter craters can be distinguished, but the 0.32 meter craters are not visible. In the 300 m lidar data, the 1.5 and 1.0 meter diameter craters are better defined, and the group of 0.32 meter craters begins to be seen as a single depression. None of the lidar data sets showed the 0.32 meter craters individually.

At the Victorville site, only one orthophoto data set was acquired. For the lidar data, the data from the 300 m and 450 m lidar flights were successfully aligned to create a combined data set, yielding a total of three lidar data densities (Figure 3-22). As at Kirtland, the data showed that feature definition increased with increasing lidar density.

**Figure 3-22**
**Victorville Test Craters, Lidar Surface Models**

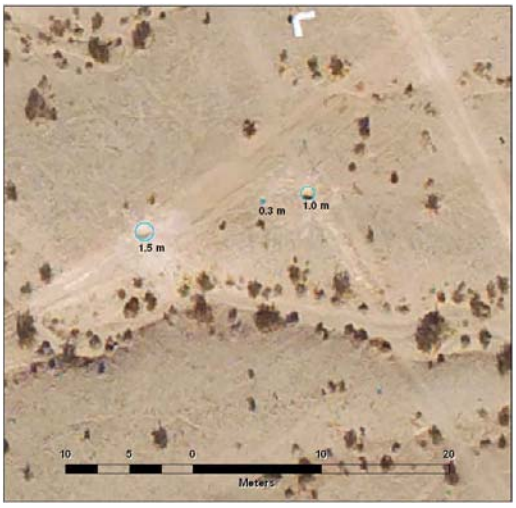


Victorville test craters – 10 cm orthophotos.

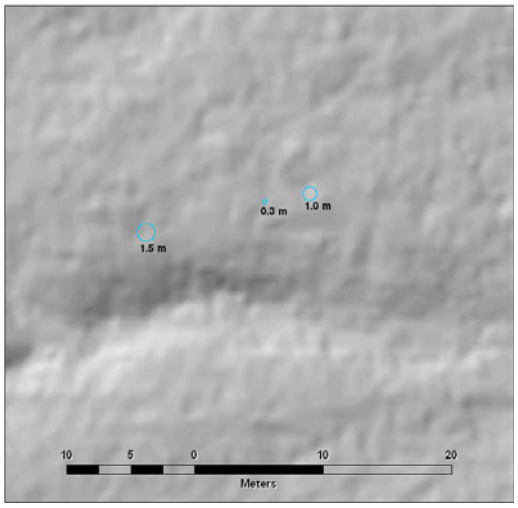


Victorville site test craters – 450 m (4.8 pts/ $m^2$) lidar flight, ground points only.

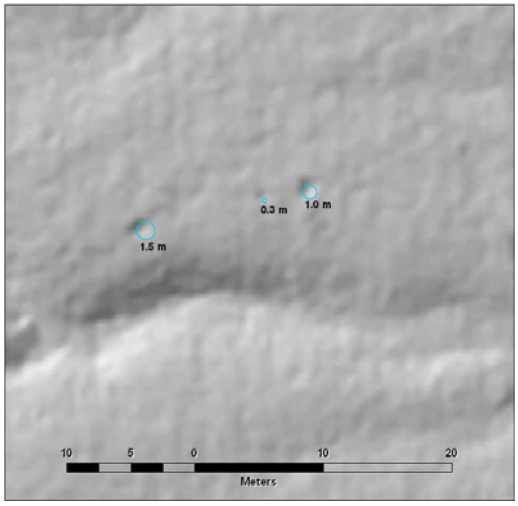


Victorville site test craters – 300 m (6.4 pts/ $m^2$) lidar flight, ground points only.

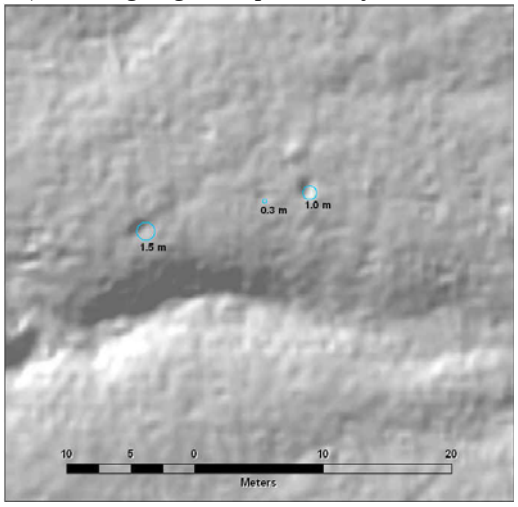


Victorville site test craters, combined (11.2 pts/ $m^2$) lidar data set, ground points only.

These images support the findings at the Kirtland site that increased lidar data density leads to better detection of smaller features. The Victorville test craters are somewhat harder to distinguish from the surrounding area because they are not grouped together. At the lower data density of the 450 m flight, the 1.0 and 1.5 m craters are difficult to distinguish, while both are clearly visible in the 300 m data and the combined data. The 0.32 m crater is discernable in the combined data set; however, without a group of craters in a regular pattern such as at Kirtland, it would be difficult to distinguish from the surrounding natural variation in the ground surface.

### 3.7.14 Data Density Effects - Quantitative Results

Counts were made of potential features identified in each lidar and orthophoto data set. For the Kirtland site, two classes of features were found: line features such as roads, trails and the target bull's-eye rings, and area features such as probable craters, isolated depressions that did not appear to be craters, and other items of interest including regularly-shaped mounds (Figure 3-23). The orthophotos area features included what appeared to be old building foundations and articles of debris on the surface. Table 3-6 presents results for each data set.

**Figure 3-23**
**Kirtland Sample Features of Interest**

Debris on the ground, approximately 1.0 x 0.5 m

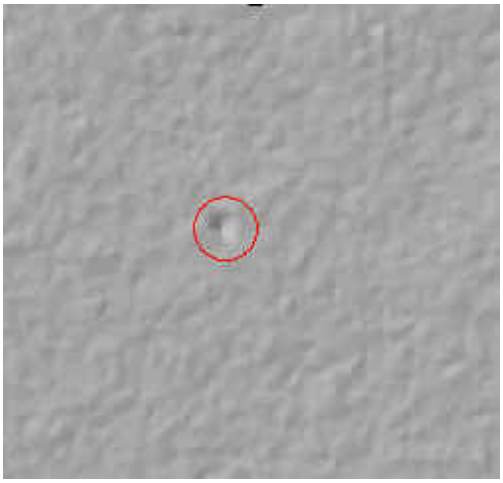

Unidentified depression, approximately 2 m in diameter

Table 3-6 summarizes the number of features identified for each data set at the Kirtland site. Figures 3-24 and 2-25 show the number of area features and the overall length of linear features detected for each orthophoto and lidar data set.

Area features included depressions that did not appear to be craters, probable craters, and other features of interest. Linear features were primarily dirt roads and jeep trails. The relatively small number of roads and trails at the Kirtland site, along with their faint and eroded character, make them appropriate subjects for comparison of the different data sets. Total length of features was used in place of the number of features to avoid problems with potentially arbitrary division of the roads and trails into segments.

**Table 3-6**
**Kirtland Potential Features**

| | Area Features | | | | Line Features |
|---|---|---|---|---|---|
| | **Depressions** | **Probable Craters** | **Other Features of Interest** | **Total Area Features** | **Total Length of Line Features (m)** |
| **Orthophotos** | | | | | |
| 20 cm | 0 | 0 | 29 | 29 | 92,325 |
| 10 cm | 0 | 0 | 49 | 49 | 83,658 |
| **Individual lidar** | | | | | |
| 900 m | 23 | 31 | 16 | 70 | 78,047 |
| 450 m | 30 | 48 | 20 | 98 | 89,907 |
| 300 m 1 | 52 | 63 | 23 | 138 | 97,968 |
| 300 m 2 | 56 | 61 | 29 | 146 | 98,220 |
| **Combined lidar** | | | | | |
| 450 and 900 m | 36 | 44 | 23 | 103 | 89,948 |
| Both 300 m | 51 | 49 | 29 | 129 | 89,974 |
| All lidar | 44 | 47 | 29 | 120 | 84,588 |

**Figure 3-24**
**Kirtland Area Features by Data Source**

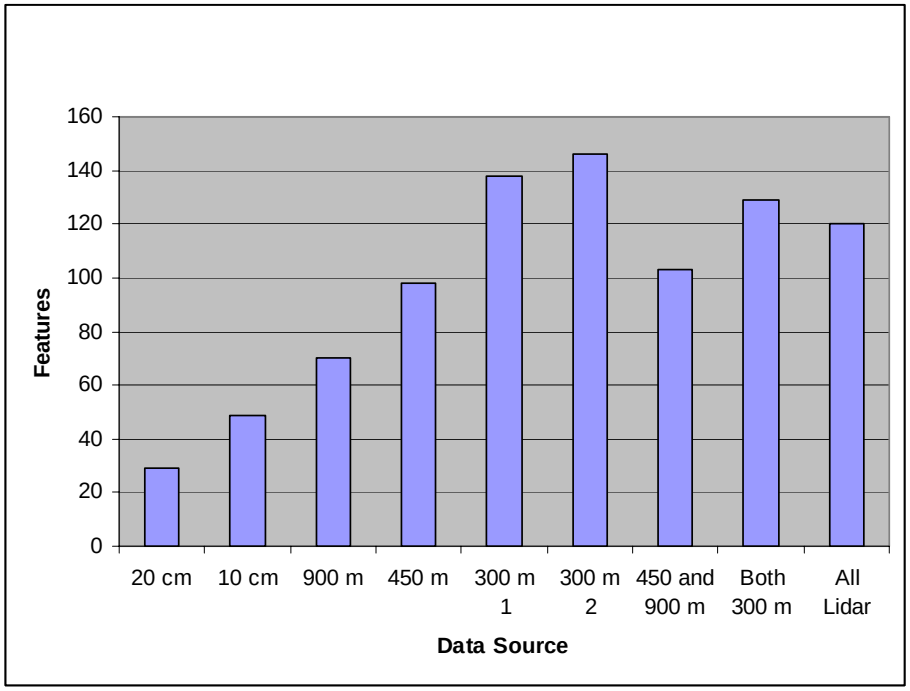

**Figure 3-25**
**Kirtland Line Feature Length by Data Source**

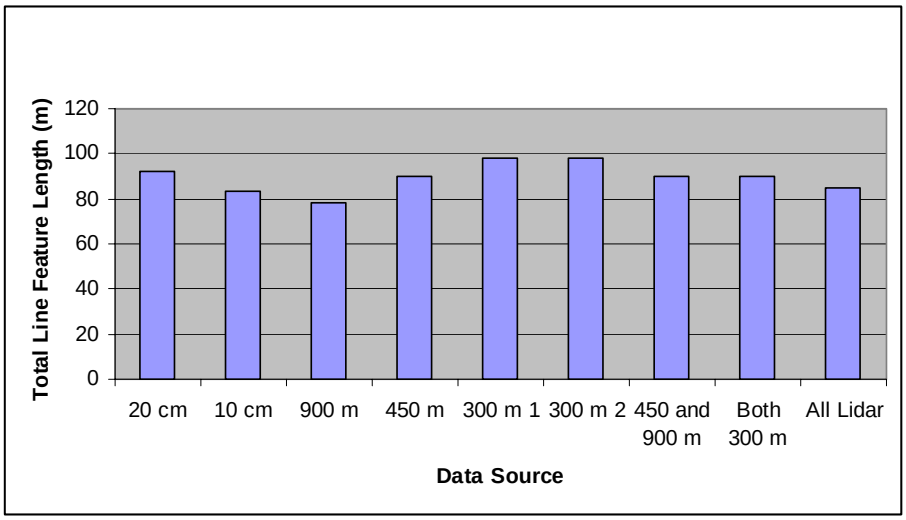


The data show that the number of area features such as potential craters was higher for lidar than for orthophotos, and the number of features identified increased with data density for both lidar and orthophotos. However, when lidar data from different altitudes was combined, the number of features detected decreased. Line features were detected roughly equally using either technology.

At the Victorville site, results were more equal between the two technologies, probably due to the larger size of the craters (Table 3-7). A slightly smaller number of craters was counted using the orthophotos, probably as a result of the vegetation in some parts of the Means Dry Lake bed that obscured the craters in the orthophotos but not the lidar data. A slightly higher number of additional features were identified using both the orthophotos and lidar together.

**Table 3-7**
**Victorville Potential Features**

| | Total Features | Probable Craters |
|---|---|---|
| **Orthophoto** | | |
| 10 cm | 1171 | 1108 |
| **Lidar** | | |
| 450 m | 1185 | 1108 |
| 300 m | 1183 | 1106 |
| 300 and 450 m | 1186 | 1105 |
| **Orthophoto and lidar** | 1198 | 1121 |

Figure 3-26 shows the number of area features for each orthophoto and lidar data set at the Victorville site.

**Figure 3-26**
**Victorville Features by Data Source**

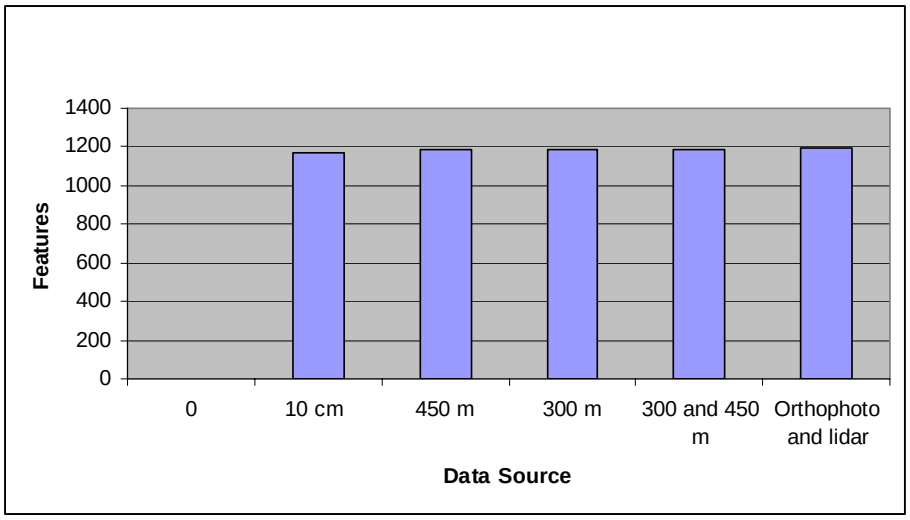


Line features were not quantitatively analyzed at Victorville, as the site is covered with off-road vehicle tracks at a density that made quantitative analysis difficult. However, roads and off-road vehicle tracks are clearly visible in both the lidar and orthophoto data at all data densities obtained.

### 3.7.15 Flight Line Orientation Effects

At the Kirtland site, the two 300 m lidar flights were flown perpendicular to each other in the north portion of the site (Figure 3-27). The resulting surface models were compared to determine whether flight line orientation would affect feature detection. The data showed that faint jeep roads running east-west were more clearly visible when the lidar flight lines are also east-west. This effect appears to be due to the orientation of the sweep of the laser either along or across these shallow roads. More distinct features, such as the larger north-south road in the images below, were equally visible in both data sets.

**Figure 3-27**
**Kirtland Flightline Orientation Effects**

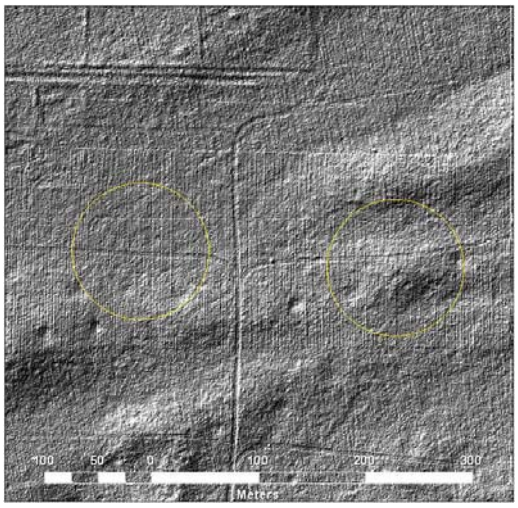


Roads, 300 m lidar east-west flight lines. Arrow shows flight line direction. East-west roads appear more clearly.

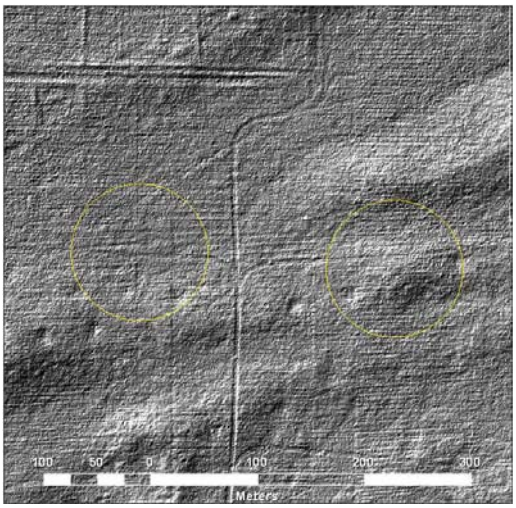


Roads, 300 m lidar, North-south flight lines. Arrow shows flight line direction. East-west roads appear less clearly.

### 3.7.16 Data Artifacts and Noise Effects

Two types of data artifacts were encountered in the lidar data. First, where data from two parallel flight lines overlapped, the surface occasionally showed very shallow (roughly 0.05 m) meandering linear features. This is a well-known type of noise effect caused by slight discrepancies between data between the two flight lines. The linear feature appears at the boundary of the overlap of the flight line overlap area (Figure 3-28). Such anomalies are probably the result of small errors in the GPS, IMU, and laser range finder that cannot be adjusted out during data processing.

**Figure 3-28**
**Kirkland Flight Line Data Overlap Effect**

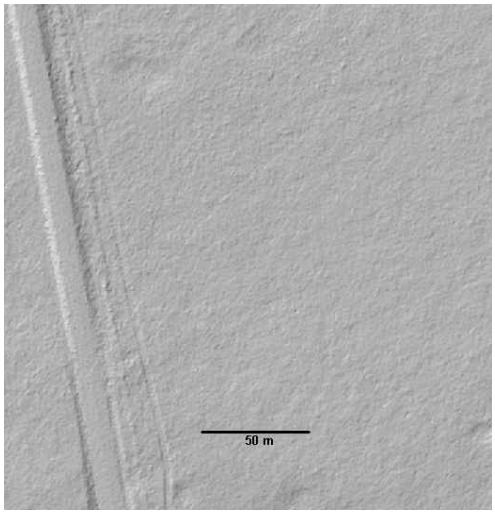


Flight line artifact, 300 m lidar. The faint linear feature shown does not appear in lidar surfaces with different flight line orientations.

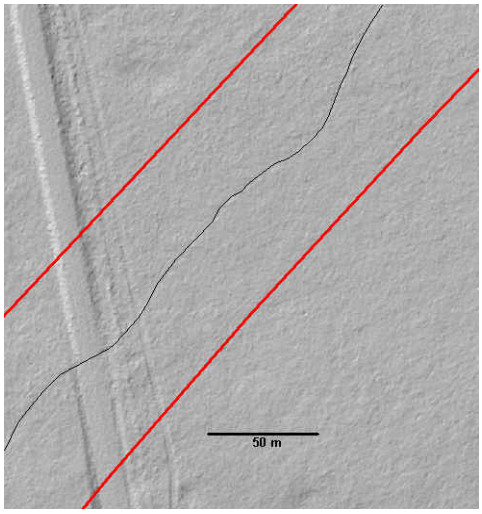


Flight line artifact, bold red lines represent flight lines.

Second, the lidar-derived ground surface often showed a “corduroy” effect consisting of shallow (roughly 0.05 m) ridges running perpendicular to the flight line and along the sweep of the laser (Figure 3-29). This is also a well-known lidar data artifact. This effect also likely results from small errors in the GPS, IMU and laser range finder. The size of both anomalies is well within the vertical accuracy specifications for the data.

**Figure 3-29**
**Victorville Lidar "Corduroy" Effect**

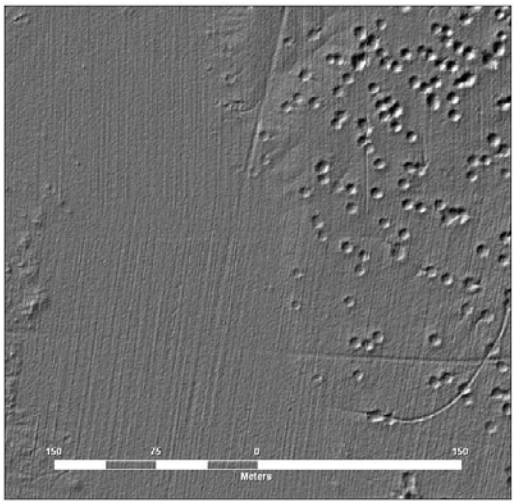


### 3.7.17 Vegetation Patterns

Vegetation at the Kirtland site was examined in both orthophotos and lidar data to determine whether vegetation patterns could reveal surface disturbances related to munitions use (Figure 3-30). Orthophotos were examined visually, and for the lidar data, vegetation heights were modeled. The bombing targets were occasionally very slightly discernable in the lidar vegetation height models; however, it is unlikely that vegetation data alone could be used to locate MRS or munitions-related features.

**Figure 3-30**
**Kirtland Vegetation Patterns**

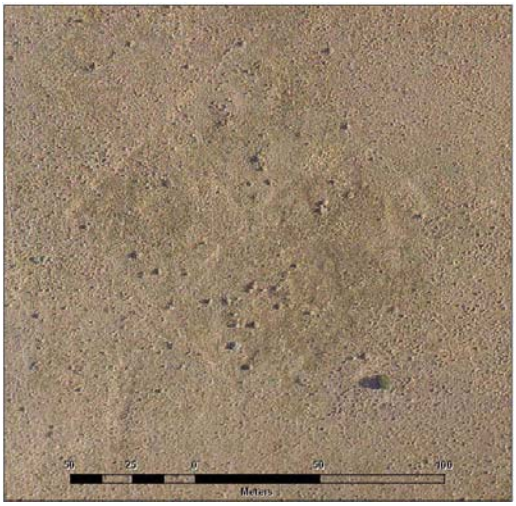


Target N3, diamond-shaped target to the west of main target area, 20 cm orthophoto.

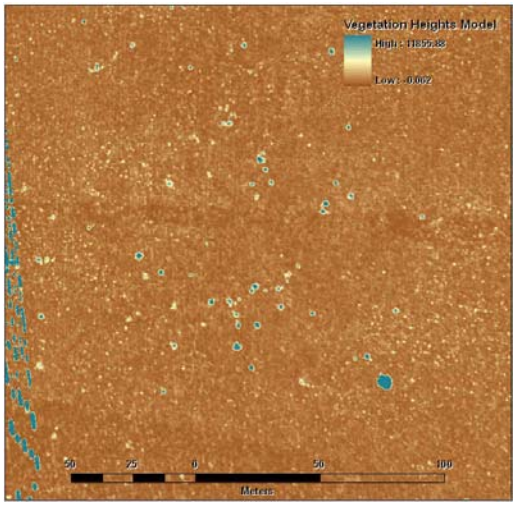


Target N3, diamond-shaped target to the west of main target area, lidar vegetation height model. The radiating bars to the west are power lines.

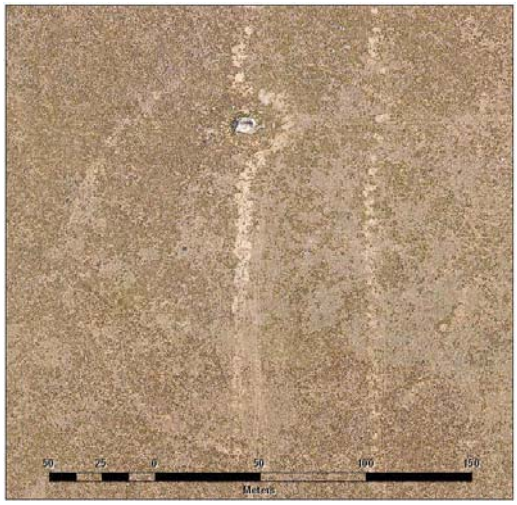


Target N2, bull's-eye.

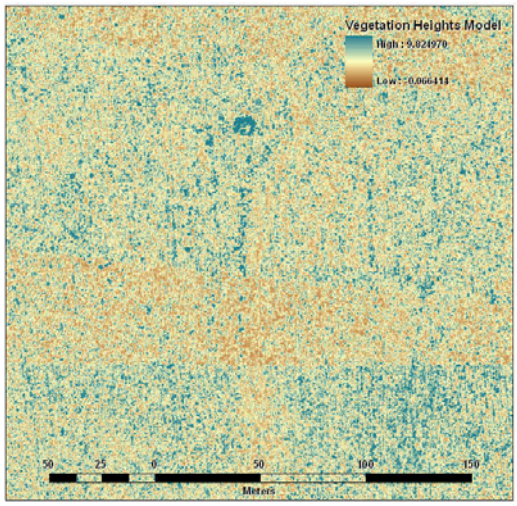


Target N2, bull's-eye, lidar vegetation height model.

### 3.7.18 Lidar and Orthophoto Positional Accuracy

Understanding the positional accuracy of lidar and orthophoto data is important since both data sets will be integrated with a wide variety of other spatial data. Positional accuracy specifications were established in the Demonstration Plan for each site, and are shown in Table

4-1 in Section 4. Positional accuracy verification methods are discussed in detail in Appendix A, Lidar and Orthophoto Positional Accuracy Results.

Lidar and orthophoto data met the positional accuracy criteria at both sites. Table 3-8 presents the overall positional accuracy results for the two sites.

**Table 3-8**
**Overall Positional Accuracy Results**

| Item | Performance Criteria | Method | Results (m) |
|---|---|---|---|
| Lidar vertical accuracy | Ave. dz: +/- 0.15 m compared to control points | Kirtland: lidar to ESTCP control points | Ave. dz: 0.111 |
| | | Kirtland: lidar to TRSI control points | Ave. dz: 0.088 |
| | | Victorville: lidar to TRSI control points | Ave. dz: 0.102 |
| Lidar horizontal accuracy | Ave. dx/y: +/- 0.65 m compared to control points | Kirtland: Average x and y displacement (dx and dy) for all control points and all lidar flights. | Ave. dx: 0.080<br>Ave. dy: 0.080 |
| | | Victorville: Average x and y displacement (dx and dy) for all control points for each flight. | 300 m flight<br>Ave. dx: 0.030<br>Ave. dy: 0.080<br>450 m flight<br>Ave. dx: 0.060<br>Ave. dy: 0.030 |
| Orthophoto horizontal accuracy | Ave. dx/y under 3 pixel widths compared to control points | Kirtland 20 cm orthophotos to control points | Ave. dx: 0.128<br>Ave. dy: 0.139 |
| | | Kirtland 10 cm orthophotos to control points | Ave. dx: 0.077<br>Ave. dy: 0.106 |
| | | Victorville 10 cm orthophotos to control points | Ave. dx: 0.027<br>Ave. dy: 0.037 |
| Orthophoto to lidar alignment | Ave. dx/dz under 2 pixel widths | Kirtland 20 cm orthophotos to lidar positions | Ave. dx: 0.167<br>Ave. dy: 0.360 |
| | | Kirtland 10 cm orthophotos to lidar positions | Ave. dx: 0.137<br>Ave. dy: 0.167 |
| | | Victorville 10 cm orthophotos to lidar positions | Ave. dx: ~0.10<br>Ave. dy: ~0.10 |

### 3.7.19 Other Observations

Orthophotos were especially useful for providing additional information about potential surface features. In Figure 3-31, orthophotos were able to clarify a feature that appeared to have moved between two lidar flights. Orthophotos showed that the feature was related to construction and had in fact moved.

**Figure 3-31**
**Use of Orthophotos to Resolve Apparent Lidar Data Discrepancy**

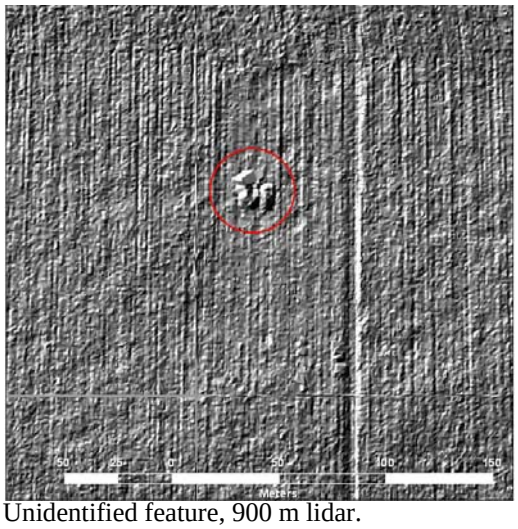

Unidentified feature, 900 m lidar.

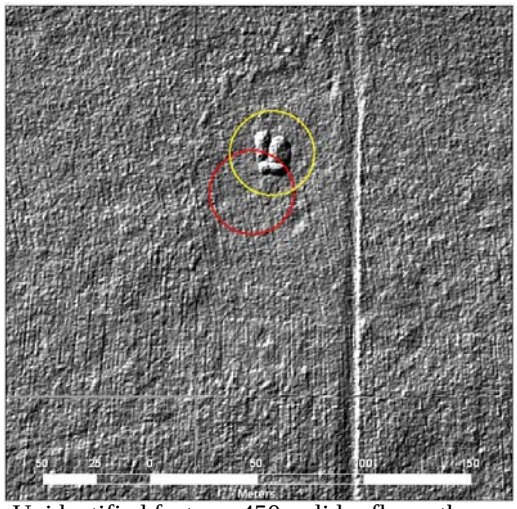

Unidentified feature, 450 m lidar flown the following day. The feature appears to have moved.

Unidentified feature, 20 cm ortho taken with the 900 m lidar flight, the orthophoto reveals that the feature is related to ongoing construction activity.

Unidentified feature, 10 cm ortho taken with the 450 m lidar flight.

# 4.0 PERFORMANCE ASSESSMENT

## 4.1 PERFORMANCE CRITERIA

Performance criteria for this demonstration were established in the Demonstration Plan for each site, and are shown in Table 4-1. The lidar and orthophoto data met these performance criteria, as shown in Tables 4-2 and 4-3. The results of validation activities and the implications of the validation results discussed in Section 4.2.

**Table 4-1**
**Performance Criteria**

| Performance Criteria | Description | Primary or Secondary |
|---|---|---|
| **Pre-mobilization** | | |
| Verification of survey control point positions | Verify survey control point locations within at least 3rd order accuracy | Primary |
| **Lidar data collection and processing** | | |
| Area coverage | 100% coverage for each flight | Primary |
| Lidar point density - Kirtland | Achieve overall lidar point densities of:<br>200 m flights (2) – 8 pts/$m^2$ each<br>450 m flight (1) – 3 pts/ $m^2$<br>900 m flight (1) – 2 pts/ $m^2$ | Primary |
| Lidar point density - Victorville | Achieve overall lidar point densities of:<br>300 m flight (1) – 3 pts/ $m^2$<br>450 m flight (1) – 5 pts/ $m^2$ | Primary |
| Lidar vertical accuracy | Vertical accuracy of +/- 15 cm compared to ground survey | Primary |
| Lidar horizontal accuracy | Horizontal accuracy of +/- 65 cm compared to ground survey | Primary |
| **Orthophoto data collection and processing** | | |
| Orthophoto area coverage | 100% coverage for each flight | Primary |
| Orthophoto flight altitude / pixel size | 450 m (for 10 cm pixel flight) – Kirtland and Victorville<br>900 m (for 20 cm pixel flight) | Primary |
| Orthophoto horizontal alignment to Lidar | Lidar and orthophotos aligned so that target features are not displaced in the two data sets | Primary |
| Orthophoto horizontal alignment to survey control points | Orthophotos aligned to survey control points so that target features are not displaced | Primary |
| **Munitions Response Site identification and analysis** | | |
| MRS identification | Correctly identify all previously identified MRS | Primary |
| MRS false alarm rate | No areas incorrectly identified as MRS | Primary |
| MRS boundary delineation | Correctly locate MRS boundaries to +/- 15% of ground-truthed area | Primary |
| MRS feature identification | Identify features presenting as munitions-related (anthropogenic) | Primary |

**Table 4-2**
**Data Quality Metrics—MRS Identification and Analysis**

| | Analytical Objective | Metric | Action to Achieve Metric | Sampling Frequency or Timing | Desired Result | Actual Result |
|---|---|---|---|---|---|---|
| **MRS Identification and Analysis** | | | | | | |
| 20 | MRS identification | Correctly identify all previously identified MRS. | Identify and document MRS from lidar and orthophoto data sets. | Each lidar and orthophoto data set and combinations. | Correctly identify all MRS. | Kirtland<br>Lidar: **Accomplished**. All previously identified MRS were correctly identified.<br>Orthophotos: **Not Accomplished.** One of four MRS correctly identified. |
| | | | | | | Victorville<br>Lidar: **Accomplished**. Both previously identified MRS were correctly identified.<br>Orthophotos: **Accomplished.** Both MRS were correctly identified. |
| 21 | MRS false alarm rate | No areas incorrectly identified as MRS. | Identify and document MRS from lidar and orthophoto data sets. | Each lidar and orthophoto data set and combinations. | No false MRS identification. | Kirtland<br>**Not Accomplished.** 15 potential MRS were identified that appear not to be munitions-related. |
| | | | | | | Victorville<br>**Accomplished.** No additional potential MRS were identified from the lidar or orthophoto data. |

**Table 4-2**
**Data Quality Metrics—MRS Identification and Analysis (continued)**

| | Analytical Objective | Metric | Action to Achieve Metric | Sampling Frequency or Timing | Desired Result | Actual Result |
|---|---|---|---|---|---|---|
| 22 | MRS boundary delineation | Correctly locate MRS boundaries to +/– 15% of ground-truthed area. | Identify and document MRS boundaries from lidar and orthophoto data sets for a selected set of test MRS. | Each lidar and orthophoto data set and combinations. | Locate MRS boundaries within metrics. | Kirtland<br>**Partially Accomplished.** For most targets, the lidar data formed the boundary of the MRS. However, at Targets N3 and SORT, additional areas were identified using mag and EM that changed the boundaries more than 15%. |
| | | | | | | Victorville<br>**Partially Accomplished.** For Target DBT Y, validation activities did not change the MRS boundary established using lidar. For Target PBR 15, mag data showed metal frag more accurately than the boundary established using lidar. |
| 23 | MRS feature identification | Identify features presenting as human-made (anthropogenic) not including craters (e.g., walls, berms, pits, small buildings). | Lidar and photo data sets will be examined for linear features. | Each lidar and orthophoto data set and combinations. | 90% of features identified from selected field-identified features. | **Accomplished.** At both sites, potential human-made features were readily identifiable. |

**Table 4-2**
**Data Quality Metrics—MRS Identification and Analysis (continued)**

| | Analytical Objective | Metric | Action to Achieve Metric | Sampling Frequency or Timing | Desired Result | Actual Result |
|---|---|---|---|---|---|---|
| 24 | MRS feature identification | Identify craters. Count 90% of craters over 1.5 m diameter and .3 m depth. | Automated algorithms will be used to identify and count craters using lidar data. | Each lidar and orthophoto data set and combinations. | 90% of craters identified outside of crater fields. 95% of craters identified inside crater fields. | Kirtland<br>**Unknown.** Validation activities appear to be no more accurate than lidar and orthophotos in identifying the highly eroded craters at the site. |
| | | | | | | Victorville<br>**Unknown.** Validation activities do not appear to have been conducted to count individual craters. However, no concentrations of craters were reported in addition to those detected using lidar and orthophotos. |
| 25 | MRS feature identification | Identify vegetation patterns indicating previous disturbance. | Automated algorithms will be used to map vegetation heights and patterns from lidar data. Results will be examined for linearity or other regular shapes. Orthophotos will be examined for regular vegetation patterns. | Each lidar and orthophoto data set and combinations. | Identification of MRS. | **Not Accomplished**. Neither orthophotos nor lidar revealed patterns of vegetation indicating previous disturbance. |

**Table 4-2**
**Data Quality Metrics—MRS Identification and Analysis (continued)**

| | Analytical Objective | Metric | Action to Achieve Metric | Sampling Frequency or Timing | Desired Result | Actual Result |
|---|---|---|---|---|---|---|
| 26 | MRS feature identification | Identify established roads. | Lidar and photo data sets will be examined for linear features. | Each lidar and orthophoto data set and combinations. | 100% identification of established roads. | **Accomplished.** Roads are clearly visible using lidar and orthophoto. Jeep tracks and other faint linear features were distinguishable from major roads. |
| 27 | MRS feature identification | Identify vehicle tracks. | Lidar and photo data sets will be examined for linear features. | Each lidar and orthophoto data set and combinations. | 90% identification of field-identified vehicle tracks. | Lidar: **Unknown.** Vehicle tracks were visible using lidar data where such tracks are deeper than 5 – 10 cm. However, field validation was not conducted. Orthophotos: **Unknown**. Vehicle tracks are clearly visible including faint jeep trails. However, field validation was not conducted. |
| 28 | MRS feature identification | Identify topography that can limit access. | Lidar data sets will be used to map areas above designated slope. | Each lidar data set and combinations. | 100% identification of steep slope areas. | **Accomplished**. Slopes were successfully modeled at both sites from lidar data. |
| **Data management** | | | | | | |
| 29 | Data management | Data backup and storage to achieve redundancy and security. | Data will be backed up to separate redundant hard drives or tape drives. | Daily backup during field and data processing operations. | Data security, prevention of data loss. | **Partially Accomplished.** All data was and remains backed up to redundant hard drives. The only exception is the one orthophoto image at Kirtland that was lost, apparently during original data collection and before it was written to the hard drive in the aircraft. |

**Table 4-2**
**Data Quality Metrics—MRS Identification and Analysis (continued)**

| | Analytical Objective | Metric | Action to Achieve Metric | Sampling Frequency or Timing | Desired Result | Actual Result |
|---|---|---|---|---|---|---|
| 30 | Data transfer | Data transfer will be in appropriate formats and file sizes for ESTCP and Kirtland Air Force Base ongoing use. | Data will meet US Government Spatial Data Standard and fully comply with Versar electronic data deliverable specifications. | Each data transfer. | Data security and quality. | **Accomplished.** Data formats met ESTCP requirements. ESTCP staff requested that data not meet Spatial Data Standards, but only that it contain standard metadata files and use ESTCP-provided data codes. This was provided. |
| 31 | Data collection report | Standard flight reporting includes: calibration log, flight log, QA/QC log, and site photos<br>. | The data collection report is a standard QA/QC product. | Calibration report: each flight day. | Full reporting is a required part of contract performance. | **Accomplished.** Calibration flights were accomplished and standard pitch, roll and heading adjustment values were calculated and recorded. |
| | | | | Flight log: each flight. | Flight log: Full reporting. | **Accomplished.** Flight log data was recorded and delivered. |
| | | | | QA/QC log: each flight. | QA/QC log: Full reporting. | **Accomplished.** Flight logs and QA/QC report were provided. |
| | | | | Site photos: whole project. | Site photos: Full reporting. | **Accomplished.** Site photos were taken and delivered. |
| 32 | Data processing report | Standard data processing report includes: GPS control ties, accuracy verification report, and QA/QC report. | The data processing report is a standard QA/QC product. | Each lidar and orthophoto data set. | Full reporting is a required part of contract performance. | **Accomplished.** GPS control, accuracy verification report and QA/QC reports were delivered. |

**Table 4-2**
**Data Quality Metrics—MRS Identification and Analysis (continued)**

| | Analytical Objective | Metric | Action to Achieve Metric | Sampling Frequency or Timing | Desired Result | Actual Result |
|---|---|---|---|---|---|---|
| 33 | Metadata | Metadata to accurately describe data format and processing steps. | Data will meet US Government Spatial Data Standards and fully comply with Versar electronic data deliverable specifications including metadata standards. | Each data transfer. | Metadata meets required standards. | **Accomplished.** ESTCP staff stated that Spatial Data Standards would not apply but that metadata would be required. Standard GIS metadata files were delivered with all data. |
| 34 | QA/QC | All data and derived products will be subject to appropriate QA/QC review. | Data processing will follow the QA/QC plan described herein. | Each data transfer. | Data are valid useful for the intended purpose and defensible. | **Accomplished.** Each data deliverable was independently reviewed by the GIS Lead and a standard QA/QC form filled out and placed in the project files. |
| 35 | Data delivery | All data will be delivered in a timely and easy-to-transfer manner. | Data deliverables will be made using ftp where possible, but in all cases will be followed up with delivery on physical media, primarily external hard drives. | Each data transfer. | Meeting data deliverable deadlines. | **Accomplished.** Data was delivered on or before the dates given in the Demonstration Plan. Interim data deliveries were made by DVD or external hard drive. Final data delivery was accomplished through external hard drive. |

**Table 4-3**
**Data Quality Metrics, Individual Performance Measures**

| | Analytical Objective | Metric | Action to Achieve Metric | Sampling Frequency or Timing | Desired Result | Actual Result |
|---|---|---|---|---|---|---|
| **Pre-flight Activities** | | | | | | |
| 1 | Study area boundary delineation | **Both Sites:** Site boundary polygon characteristics agreed on and documented to allow comparison with data collected. | Achieve stakeholder agreement to boundary parameters. | Once at beginning of program. | Document site boundary for measurement of future boundary metrics. | **Accomplished.** Boundaries were agreed on and utilized. |
| 2 | Survey control point confirmation measurement | **Both Sites:** Confirm coordinates of survey control points within at least third-order accuracy. | Perform and record GPS survey (static or kinematic). | Pre-flight (or during on-site acquisition). | Confirm coordinates of survey control points. | **Accomplished.** Control points were independently occupied by TRSI and ESTCP. |
| **Lidar Data Collection and Processing** | | | | | | |
| 3 | Sensor calibration | **Both Sites:** Resolve roll/pitch/ heading for installation. | Perform opposing direction and orthogonal passes over baseline. Compare with nominal values from standard installation. | Prior to each flight day. | +/– 0.02 degrees | **Accomplished.** Standard roll, pitch and heading correction factors were established through calibration flights for both sites. See Appendix A. |
| 4 | Sensor speed | **Both Sites:** Laser pulse rate between 50 and 100 kHz. | Set laser pulse speed and the altitude of the low lidar passes depending on site conditions to achieve highest possible point density. | Prior to each flight day. | Achieve target sensor speed. | **Accomplished.** Laser pulse rate of 50 kHz was used at both sites. |

**Table 4-3**
**Data Quality Metrics, Individual Performance Measures (continued)**

| | Analytical Objective | Metric | Action to Achieve Metric | Sampling Frequency or Timing | Desired Result | Actual Result |
|---|---|---|---|---|---|---|
| 5 | Flight altitude, Kirtland | **Kirtland:** Flight altitudes of 900, 450, and 200 to 300 m. | Establish and fly appropriate flight altitudes for the desired lidar point densities and orthophoto pixel sizes. Lay out a series of flight lines for high-density lidar collection to be able to respond to site conditions. | Each flight line. | +/- 50 m from planned flight altitudes. | **Accomplished.** Lidar flight altitudes were 900, 450 and 300 m. Flight altitudes are documented through daily flight logs. |
| | Flight altitude, Victorville | **Victorville:** Flight altitudes of 450 and 300 m. | Establish and fly appropriate flight altitudes for the desired lidar point densities and orthophoto pixel sizes. Lay out a series of flight lines for high-density lidar collection to be able to respond to site conditions. | Each flight line. | +/- 50 m from planned flight altitudes. | **Accomplished.** Lidar flight altitudes were 900, 450 and 300 m. Flight altitudes are documented through daily flight logs. |
| 6 | Area coverage | **Both Sites:** 100% coverage for each flight. | Establish and fly flight lines so as to cover the entire target area. Data from each day's flights will be examined and data gaps will be filled. | Each flight. | 100% coverage. | **Accomplished**. 100% coverage of the study area was accomplished for each flight at both sites. |
| | | | | | 15% flightline overlap, 50m over area boundaries. | **Accomplished.** Flight line overlap met specifications for all flights. |

**Table 4-3**
**Data Quality Metrics, Individual Performance Measures (continued)**

| | Analytical Objective | Metric | Action to Achieve Metric | Sampling Frequency or Timing | Desired Result | Actual Result |
|---|---|---|---|---|---|---|
| 7 | Data collection rate | **Both Sites:** Collect data for the entire site within the established schedule. Reserve one additional day for QA/QC and re-flight. | Establish and review flight lines and flight schedule prior to data collection. | NA | Full data collection within planned schedule. | **Partially Accomplished**. Data was acquired as planned at Kirtland. At Victorville, data collection required two additional days due to high ambient air temperature. |
| 8 | Lidar point density | Achieve overall densities of: | Plan and accomplish appropriate sensor speed, flight altitude, and air speed. Flights more than 10% below target point densities will be repeated. | Each flight. | Data collection within 10% of target densities. | **Partially Accomplished.** At Kirtland, data for the 900 m and 450 m flights met or exceeded target densities. Data was below target density for the low-level flights. Lower densities resulted from 50 kHz laser pulse rate combined with 300 m flight altitude. At Victorville, data met target densities. |
| | | Kirtland I<br>200 m flights (2) – 8 pts/m$^2$ each | | | 200 m flights (2) – 8 pts/m$^2$ each | N block flight 1: 5.2 pts/m$^2$<br>N block flight 2: 6.5 pts/m$^2$<br>S block flight 1: 5.9 pts/m$^2$<br>S block flight 2: 6.1 pts/m$^2$ |
| | | Kirtland II<br>450 m flight (1) – 3 pts/m$^2$ | | | 450 m flight (1) – 3 pts/m$^2$ | N block: 5.2 pts/m$^2$<br>S block: 4.1 pts/m$^2$ |
| | | Kirtland III<br>900 m flight (1) – 1.5pts/m$^2$. | | | 900 m flight (1) – 1.5pts/m$^2$. | N block: 1.4 pts/m$^2$<br>S block: 1.6 pts/m$^2$ |

**Table 4-3**
**Data Quality Metrics, Individual Performance Measures (continued)**

| | Analytical Objective | Metric | Action to Achieve Metric | Sampling Frequency or Timing | Desired Result | Actual Result |
|---|---|---|---|---|---|---|
| | | Victorville I 300 m flight – 6 pts/$m^2$ | | | 300 m flight – 6 pts/$m^2$ | 6.4 pts/$m^2$ |
| | | Victorville II 450 m flight – 4.5 pts/$m^2$ | | | 450 m flight – 4.5 pts/$m^2$ | 4.8 pts/$m^2$ |
| 9 | Lidar flight line alignment | **Kirtland** The two 200 m flights will be orthogonal. | Appropriate flight lines will be designed and flown. Planned flight lines will be submitted in advance. | Each flight. | Flight lines within $10^o$ of orthogonal. | **Partially Accomplished.** North block flights were orthogonal. South block flights were both flown northeast-southwest. The Double Eagle airport runway is just north of the south block. North-south flight lines would have required crossing and turning directly over the airstrip, which was impossible for safety reasons. |
| | | **Victorville:** The 300 m and 450 m flights will be orthogonal. | Appropriate flight lines will be designed and flown. Planned flight lines will be submitted in advance. | Each flight. | Flight lines within 10° of orthogonal. | **Accomplished.** The two flights were flown orthogonal. |

**Table 4-3**
**Data Quality Metrics, Individual Performance Measures (continued)**

| | Analytical Objective | Metric | Action to Achieve Metric | Sampling Frequency or Timing | Desired Result | Actual Result |
|---|---|---|---|---|---|---|
| 10 | Lidar vertical accuracy | **Both Sites:** Vertical accuracy of +/– 15 cm compared to ground survey. | Steps: | Each flight | | |
| | | | 1. Perform sensor calibration as described above | | As above. | **Accomplished.** |
| | | | 2. Obtain ground elevations on identifiable points using ground based GPS methods (static and/or kinematic) | | As above. | **Accomplished.** Control points were collected as described. |
| | | | 3. Compare ground-based and airborne elevations. | | Meet or exceed +/1 15 cm lidar to control point vertical accuracy. | **Accomplished.** Elevation comparisons were performed between control point elevations and the interpolated elevation of the lidar surface at that point. Results were within specifications. See Appendix A. |
| 11 | Lidar horizontal accuracy | **Both Sites:** Horizontal accuracy of +/– 65 cm compared to ground survey. | Steps: | Each flight. | | **Accomplished.** Positions of control points were obtained in the Lidar data using intensity values. These positions were compared to the surveyed locations of these control points. Horizontal accuracy was well within specification. See Appendix A. |
| | | | 1. Perform sensor calibration as described above | | As above. | **Accomplished.** |

**Table 4-3**
**Data Quality Metrics, Individual Performance Measures (continued)**

| | Analytical Objective | Metric | Action to Achieve Metric | Sampling Frequency or Timing | Desired Result | Actual Result |
|---|---|---|---|---|---|---|
| | | | 2. Obtain ground positions on identifiable points using ground based GPS methods (static and/or kinematic) | | As above. | **Accomplished.** |
| | | | 3. Compare ground-based and airborne positions. | | Meet or exceed +/- 65 cm lidar to control point horizontal accuracy. | **Accomplished.** |
| 12 | Lidar data integration – flight lines | **Both Sites:** Achieve flight line to flight line edge match of +/– 12cm. | Review statistics from lidar processing software. | Line to line. | Achieve best possible match between individual lidar flight lines. | **Accomplished.** |
| 13 | Lidar point separation | **Both Sites:** Remove 100% of large features, (trees, buildings, vehicles) | Operators remove non-ground laser returns through automated separation routines followed by hand cleaning and inspection. | Lidar data set for each flight. | Satisfactory visual inspection of surface model of the ground surface. | **Accomplished.** Lidar points were classified as ground and non-ground returns. Visual inspection of the ground returns showed that all buildings, fences, and other larger features were successfully removed. |
| | | Remove small features (grass, low brush) to the level where remaining data cannot distinguish ground from non-ground features. | | | Satisfactory visual inspection of surface model of the ground surface. | **Accomplished.** Inspection of ground and non-ground lidar points in conjunction with orthophotos showed that small brush and tall grass was removed within specification. |

**Table 4-3**
**Data Quality Metrics, Individual Performance Measures (continued)**

| | Analytical Objective | Metric | Action to Achieve Metric | Sampling Frequency or Timing | Desired Result | Actual Result |
|---|---|---|---|---|---|---|
| | **Orthophoto Data Collection and Processing** | | | | | |
| 14 | Orthophoto area coverage | **Both Sites:** 100% coverage for each flight. | Wireframes of "raw" images are compared to the project boundary to check for gaps or holes. | Each flight day as part of QA/QC checks. | 100% coverage with sufficient image overlap for ortho-rectification. | **Partially Accomplished.** At Kirtland, complete coverage was obtained for both flights with the exception of one image in the 10 cm flight. The missing image is approximately 125 x 200 meters, located on the north boundary of the study area. The file appears to have been corrupted during collection. At Victorville, complete coverage was obtained. |
| 15 | Orthophoto flight altitude/ pixel size | Kirtland I 450 m (for 10 cm pixel flight) | Orthophoto pixel size is directly related to flight altitude. Flight lines are designed for the desired pixel sizes. Flight data will be examined during and after each flight and flight lines outside of the range will be repeated. | Each flight. | Achieve specified flight altitudes and pixel sizes. | **Accomplished.** 10 cm pixel sizes were achieved for 100% of the study area with the exception of the one missing image. |

**Table 4-3**
**Data Quality Metrics, Individual Performance Measures (continued)**

| | Analytical Objective | Metric | Action to Achieve Metric | Sampling Frequency or Timing | Desired Result | Actual Result |
|---|---|---|---|---|---|---|
| | | Kirtland II<br>900 m (for 20 cm pixel flight). | | | Achieve specified flight altitudes and pixel sizes. | **Accomplished.** 20 cm pixel sizes were achieved for 100% of the study area. |
| | | Victorville<br>450 m (for 10 cm pixel flight) | | | Achieve specified flight altitudes and pixel sizes. | **Accomplished.** 10 cm pixel sizes were achieved for 100% of the study area. |
| 16 | Orthophoto image mosaicing | **Both Sites:** No obvious seams between images in the final orthophoto. | Creation of an image mosaic from individual small images is largely an operator controlled rather than an automated process. | Each orthophoto composite image (10 cm and 20 cm). | Line features are continuous with no visible discontinuity at mosaic seams. | **Accomplished.** Visual inspection of the orthophoto images showed no obvious seams. |
| 17 | Orthophoto image color balancing | **Both Sites:** No obvious color imbalances within data for each session. | Color balancing is an operator controlled process based on viewing the mosaic to identify any areas of tonal imbalance. | Each orthophoto composite image (10 cm and 20 cm). | Continuity of tone such that individual images are not visible in mosaic. | **Accomplished.** Visual inspection of the orthophoto images showed no obvious color imbalances. |
| 18 | Orthophoto horizontal alignment to lidar | **Both Sites:** Lidar and orthophotos aligned so that target features are not displaced in the two data sets. | Orthorectification is performed using the lidar data and fiducial locations are control data sources, followed by operator adjustment. | Each orthophoto composite image. | Orthophotos aligned to +/– 2 pixel widths. | **Accomplished.** Positions of control targets were compared using the orthophoto and lidar intensity values. Locations were within specifications. See Appendix A. |

**Table 4-3**
**Data Quality Metrics, Individual Performance Measures (continued)**

| | Analytical Objective | Metric | Action to Achieve Metric | Sampling Frequency or Timing | Desired Result | Actual Result |
|---|---|---|---|---|---|---|
| 19 | Orthophoto horizontal alignment to fiducials | **Both Sites:** Orthophotos aligned to survey control points so that target features are not displaced. | Orthorectification is performed using the lidar data and fiducial locations are control data sources, followed by operator adjustment. | Each orthophoto composite image. | Orthophotos aligned to +/– 3 pixel widths. | **Accomplished.** Ortho image positions were compared to control targets visible in the images. In addition, lidar and orthophoto positions were compared for building corners and edges of pavement that were visible in both the orthophoto and lidar data. Positions were within specifications. See Appendix A. |

## 4.2 PERFORMANCE CONFIRMATION METHODS

### 4.2.1 Demonstration-Level Confirmation Methods

At the demonstration level, the effectiveness of lidar and orthophotos was evaluated based on its ability to meet the stated performance criteria given in Table 4-1. The demonstration relied on proven industry methods to assure predictable results, including the use of survey controls, equipment calibration, alignment of lidar points to the survey control points and from one flight line to the next, and QA/QC checks throughout the project. Both lidar and orthophoto data met all data quality specifications.

During data analysis, standard GIS methods were used to create surface models from the lidar data. As a means to ensure objective results, staff assigned to initial feature identification was not provided with the CSM and did not know the history of munitions use at the site. All feature and MRS identification was subject to QA/QC review by project staff familiar with both the CSM and UXO/MEC generally.

### 4.2.2 Program Level Confirmation Methods

Lidar and orthophotos were evaluated for their ability to meet the goals of the WAA Pilot Program as a whole. Evaluation was based on comparing the results of the lidar and orthophoto data with the results of the other data collected at the two sites, including helicopter and transect magnetometry and transect-based EMI, along with validation data including 100% coverage magnetometry areas, site reconnaissance, and intrusive sampling. In general, these subsequent activities confirmed the findings and usefulness of lidar and orthophotos. They also revealed areas where lidar and orthophotos did not detect areas of concentrated munitions use, with implications for the appropriate use of these technologies at future sites.

For both of the sites, lidar, orthophotos, helicopter magnetometry, and towed-array magnetometry or EMI were collected on the entire demonstration site where terrain and vegetation allowed. This procedure was designed to facilitate comparison of the contributions of the various technologies in different site conditions. At production sites, it is assumed that the three technologies would be deployed in a manner that would consider time and budget constraints faced by site managers. In such a model, lidar and orthophotos would be deployed to the site first and the results used to guide the deployment of the subsequent magnetometry layers.

Validation activities included 100% coverage surveys of small parcels using the ground system, reconnaissance surveys, and a limited intrusive investigation. These were undertaken to validate both the data collected by the other technologies, and their conclusions, such as the conclusions as to the ordnance origin of features.

The reconnaissance survey team (an explosive ordnance disposal specialist and a geophysicist with a hand-held GPS and camera) located and confirmed anomalies observed in the helicopter data. The ground systems were used to survey smaller (tens of acres) patches near targets and in areas of no obvious munitions use, to determine the distributions of anomalies across the site. The intrusive investigation confirmed the identity of sub-surface features detected by the geophysical sensors and confirmed the reliability of feature classification using the geophysical results.

### 4.2.3 Results: Kirtland

At the Kirtland site, helicopter and ground-based magnetometry confirmed the ordnance origin of the MRS identified in the initial CSM. There was good general agreement between the lidar and orthophoto data and the helicopter magnetrometry data, as shown in Figure 4-1.

**Figure 4-1**
**Kirtland Helicopter Magnetometry Density Grid**

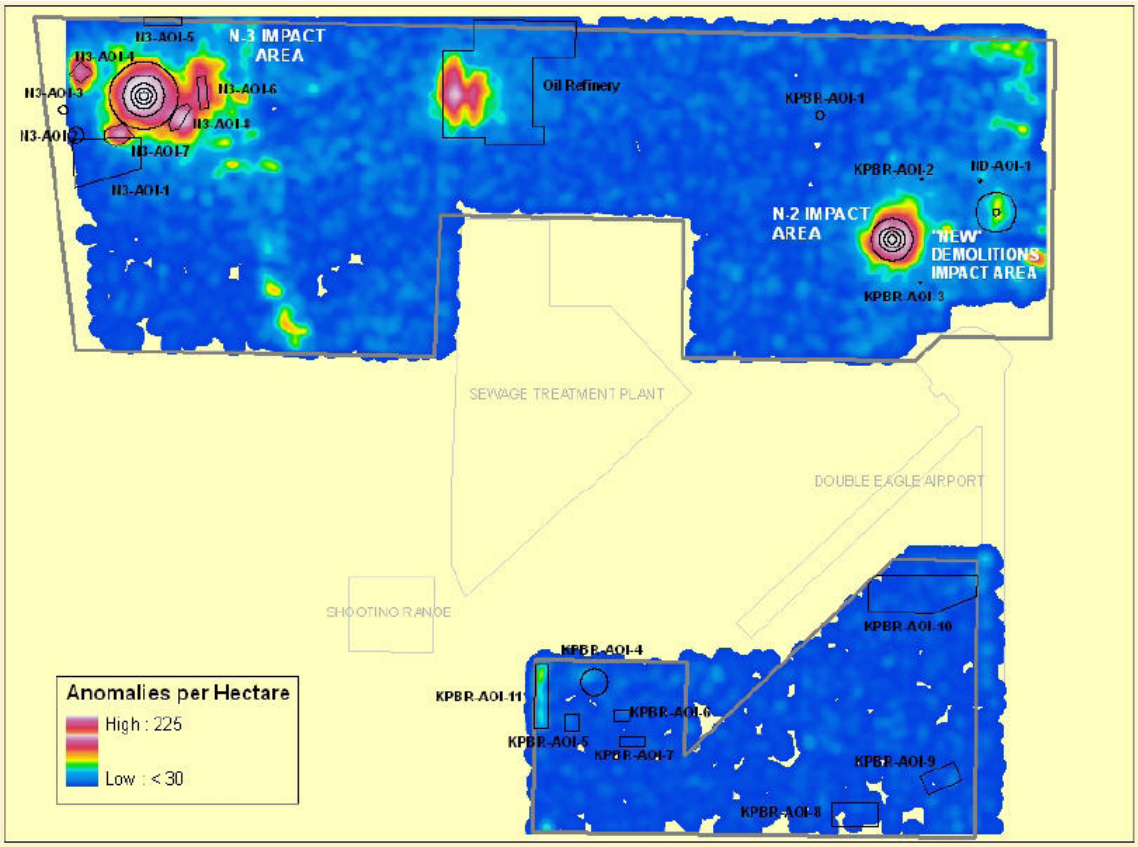


Source: ESTCP (2007a)

Results for the individual targets and areas of interest (AOIs) are discussed below.

***Target N3***

Target N3 is the most complex target area at the Kirtland demonstration site. For the main bombing target, the lidar and orthophoto data were very consistent with the validation data. Lidar and orthophoto data clearly showed the concentric circles of the bombing target. On-site reconnaissance located the target center but not the rings, which were too eroded to be visible from the ground. Helicopter magnetometry showed concentrations of anomalies within the target rings, as did the transect data. Intrusive sampling located abundant ordnance-related scrap along with four intact ordnance items.

There were no apparent craters within the aiming circles, and all ordnance-related scrap retrieved from the intrusive sampling was from 100-pound M38A2 practice rounds. The archival search report did not indicate any other munitions activity at this target. All data is consistent the CSM, which identified the area as a practice bombing target.

There were eight additional AOIs at Target N3, six of which were identified from the lidar and orthophoto data and two that were identified from the magnetometry data. The results using lidar and orthophotos, as well as from the relevant subsequent investigations are given below, using the AOI names given in the revised CSM:

- N3-AOI-1 is the possible crossed runway target southwest of the outer aiming circle. This area was identified in the lidar data as a potential additional target area. Portions of this area showed concentrations of geophysical anomalies.

- N3-AOI-2 and N3-AOI-3 were identified from the lidar data by possible craters. Site reconnaissance identified these as depressions with no evidence of ordnance scrap.

- N3-AOI-4 appears in the lidar data as a diamond-shaped potential target area west of the main target. (The CSM describes this as a “raised area shaped in a cloverleaf pattern.”) There were high concentrations of geophysical anomalies throughout the area and a large amount of ordnance-related scrap was retrieved.

- N3-AOI-5 appears in the lidar data as a long rectangular disturbance of the ground shaped like a single runway. Few anomalies were seen in the helicopter or transect magnetometry data; however, anomalies appeared in the 100% geophysical survey and some ordnance-related scrap was retrieved during the intrusive sampling.

- N3-AOI-6 appears in the lidar data ship-shaped potential target. The shape was confirmed by site reconnaissance, while geophysical data showed high concentrations

of anomalies and intrusive sampling located ordnance-related scrap and one intact ordnance item.

- N3-AOI-7 and N3-AOI-8 were not identified using the lidar or orthophoto data and were identified using helicopter magnetometry by concentrations of geophysical anomalies. Intrusive investigation showed that both areas had large amounts of ordnance-related scrap, and three intact ordnance items were located within N3-AOI-7.

The results of these activities at the AOIs are shown in Figures 4-2 and 4-3.

**Figure 4-2**
**Kirtland Target N3 and Associated AOIs**

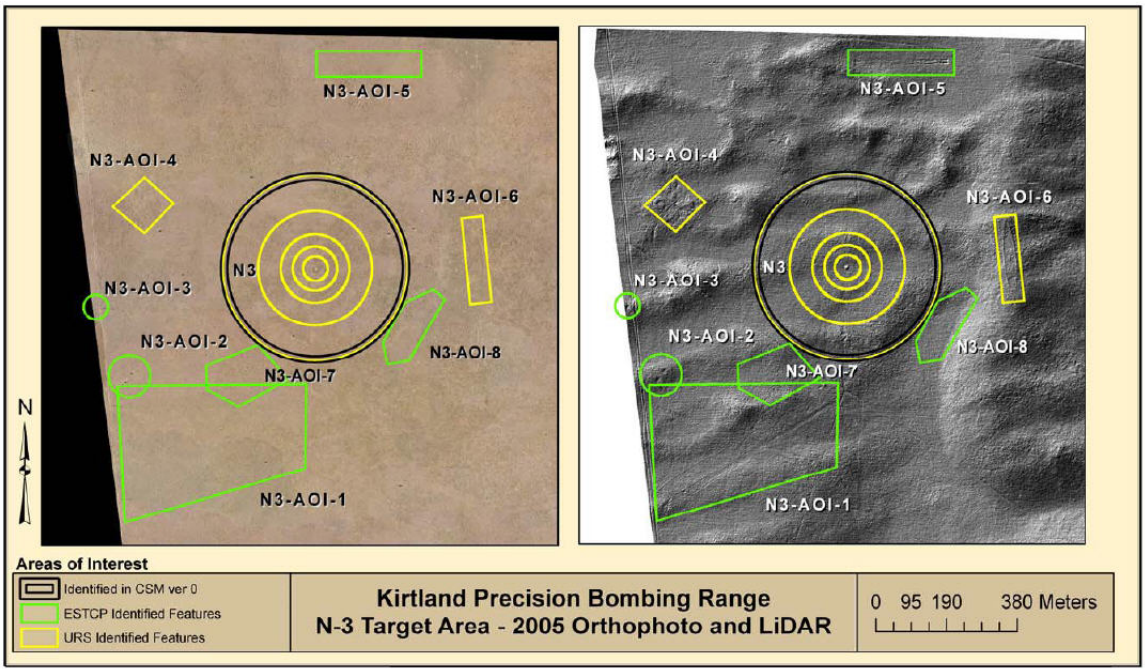


Source: ESTCP (2007a)

The location of N3-AOI-7 and N3-AOI-8, which were not detected using lidar and orthophotos, are shown, just southeast and southwest of the aiming circles.

**Figure 4-3**
**Kirtland Target N3 and Associated AOIs, Geophysics Data**

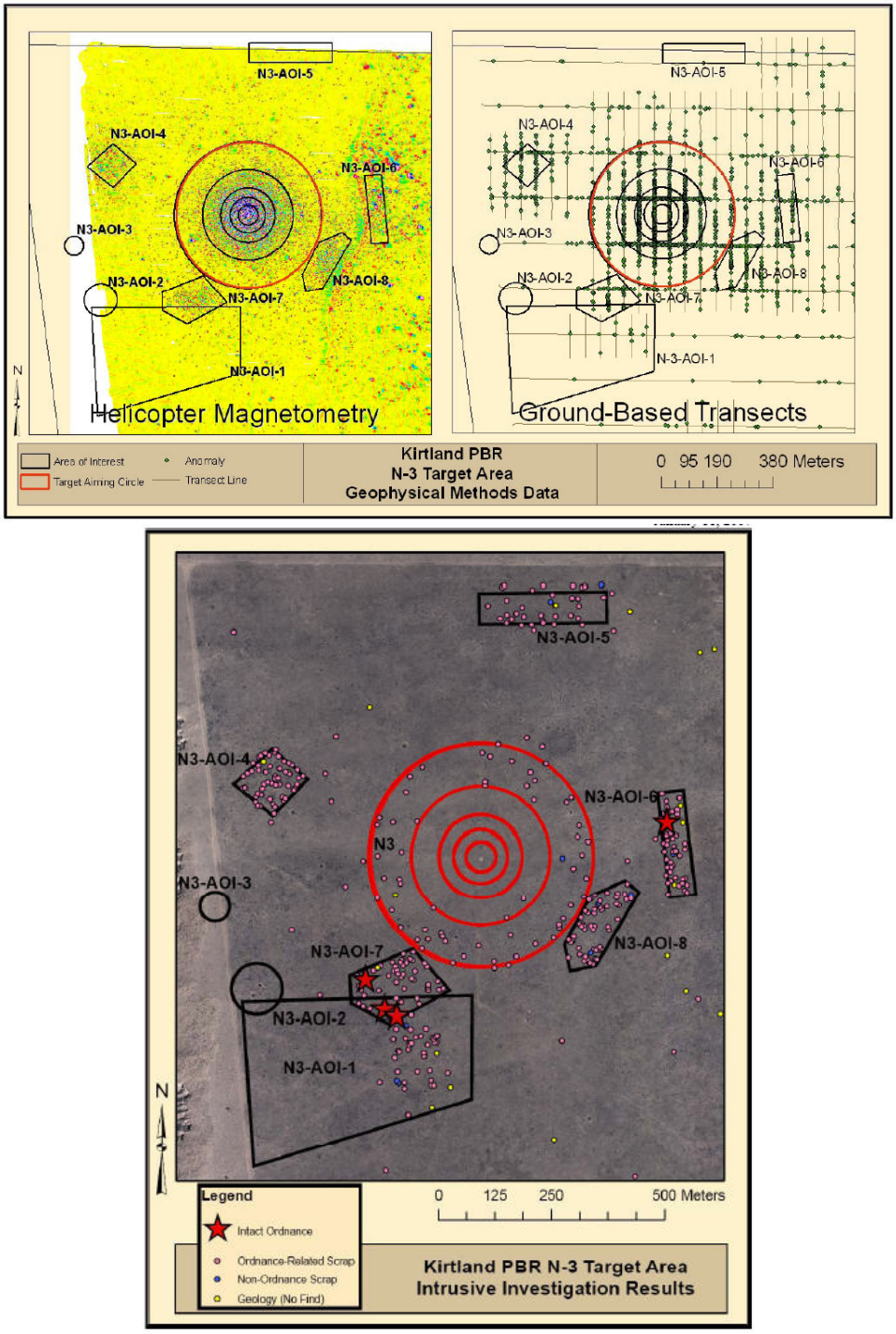


Source: ESTCP (2007a)

### *Simulated Oil Refinery*

This SORT target is described in the initial CSM as a series of cells forming a rectangular shape. The target outline shown in Figures 4-4 and 4-5 is based on interpretation of the lidar and orthophoto data, in which rectangular cells and other berms are visible. The helicopter and transect magnetometry data showed a concentration of anomalies only in the western portion of the target area. The lack of craters and the nature of the ordnance scrap recovered support the conclusion that only 100-pound practice bombs were used at this target.

**Figure 4-4**
**Kirtland Target SORT, Geophysics Data**

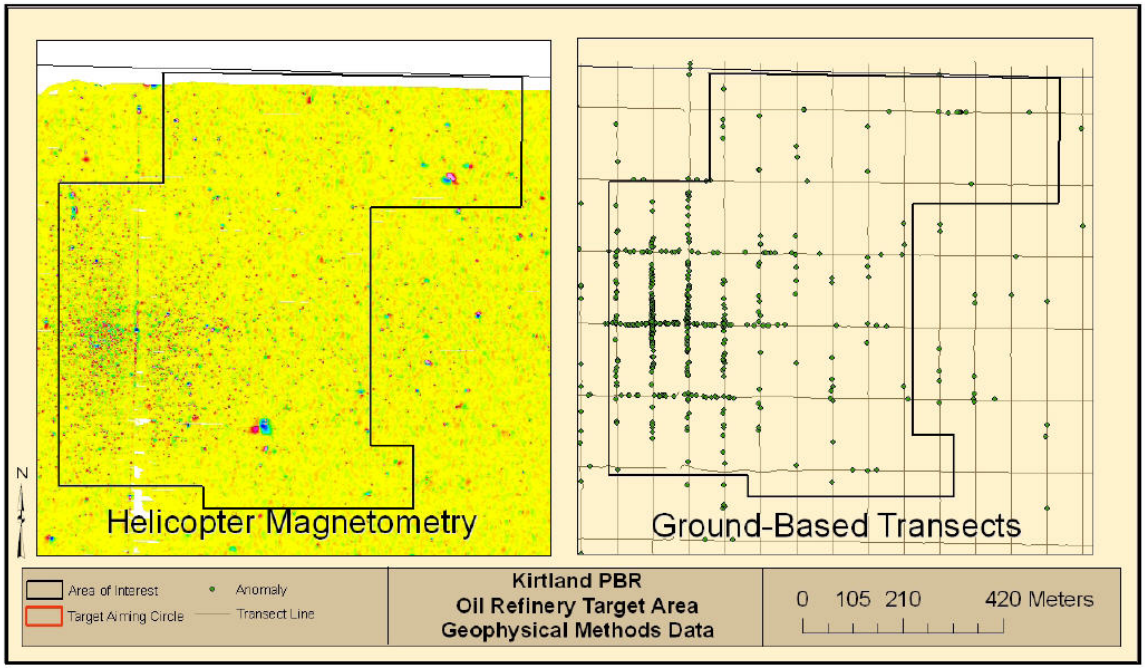


Source: ESTCP (2007a)

The transect and 100% coverage magnetometry data showed that anomalies extended past the boundaries of the target visible in the lidar and orthophoto data, though at low concentrations. Intrusive surveys confirmed that these anomalies included ordnance-related scrap, which extended to the farthest area surveyed.

**Figure 4-5**
**Kirtland Target SORT, Intrusive Investigation Results**

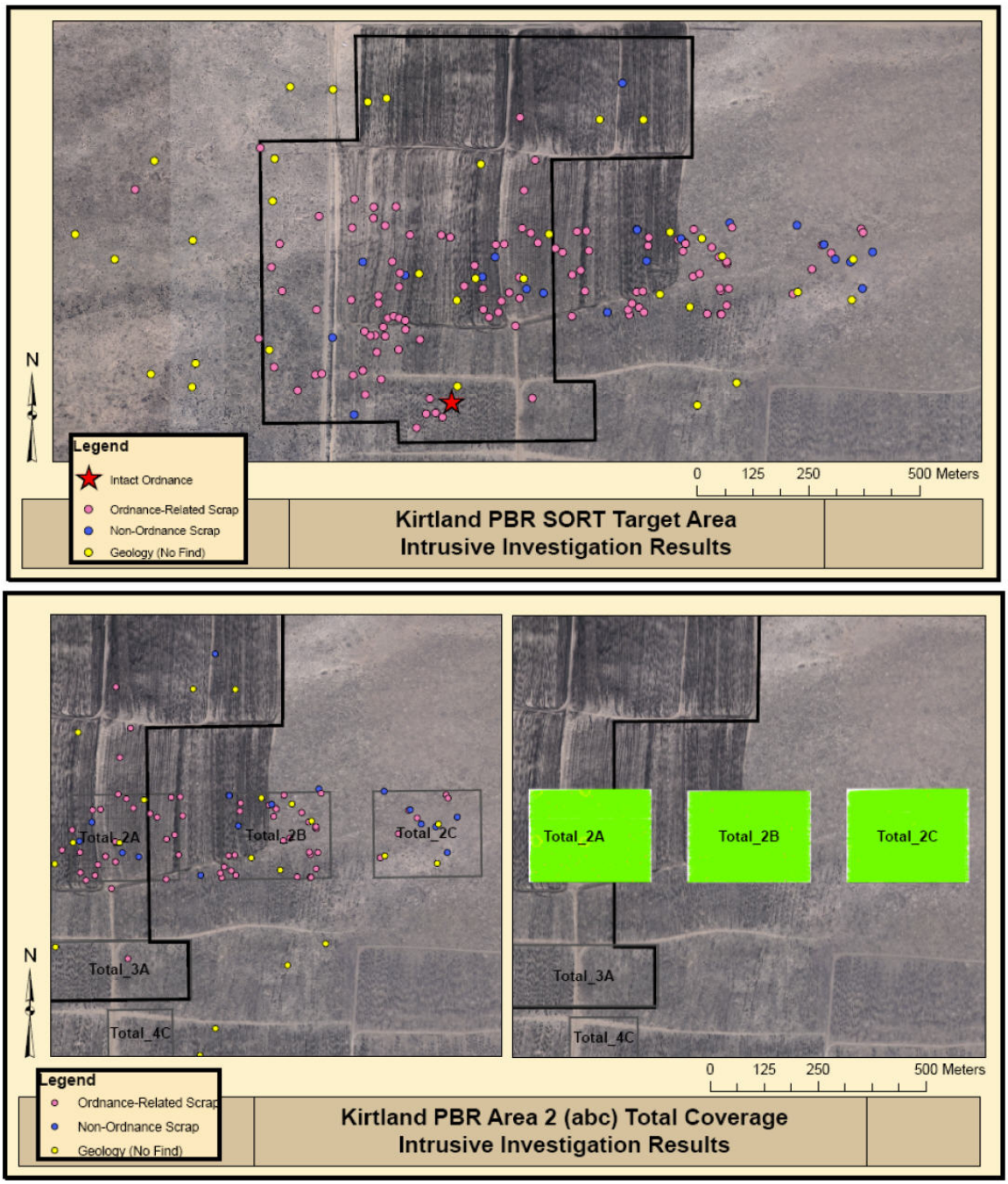


Source: ESTCP (2007a)

### *Target N2*

Target N2 is described as a 1,000-foot bull's-eye target used for 100-pound practice bombs. Lidar and orthophoto data clearly showed the concentric circles making up this bombing target, although these were not visible from ground reconnaissance. No craters were seen in either the lidar data or site reconnaissance. Helicopter and ground-based magnetometry showed high concentrations of anomalies throughout the target circle to the outer ring (Figure 4-6). A large amount of small frag and ordnance-related scrap was observed at the surface. Ordnance-related scrap retrieved as part of the intrusive investigation was all from 100-pound M38A2 practice rounds or aerial flares. This data is all consistent with the conclusion that the target was used for practice bombing.

A structure located on the second inner ring to the north of the center is visible in both the orthophotography and the lidar data. Site reconnaissance identified this a razed cinderblock building.

The results of 100% magnetometry surveys and intrusive investigation were consistent with each other. There was a high concentration of ordnance-related anomalies and objects within the target, with the density falling off with distance but not to zero. These results indicate that, as at Target SORT, even the area considered background contained some ordnance-related material.

**Figure 4-6**
**Kirtland Target N2, Geophysics Data**

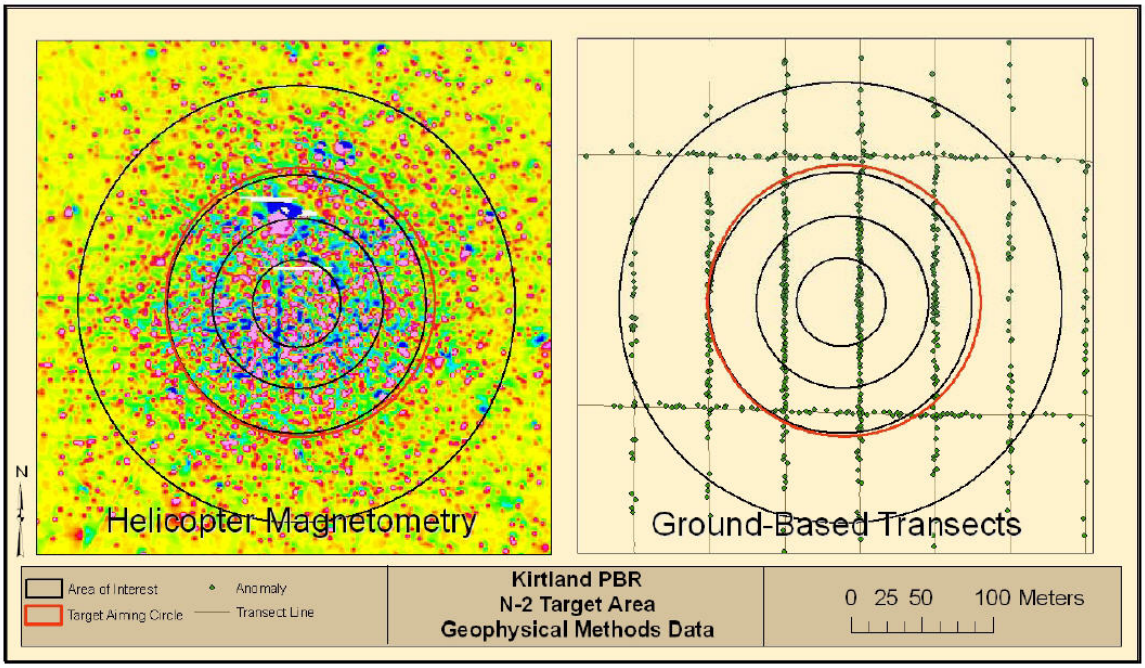


Source: ESTCP (2007a)

### *New Demolitions Impact Area*

Target NDIA is described in the initial CSM as a 1,000-foot-diameter HE bull's-eye target. The lidar data did not show any evidence of target rings, but did show numerous potential craters. The orthophoto data showed target cross-hairs and one target ring. Helicopter and transect magnetometry both showed a low density of anomalies in and near the target area (Figure 4-7). The 100% ground geophysical surveys collected through the center of the inner target circle and at the northern edge of the outer circle showed concentrated anomalies at the center, getting more sparse further away. Intrusive sampling was not performed on these anomalies due to the possible presence of 250-pound HE bombs in close proximity to the airport. Field reconnaissance located craters and heavy walled frag. Both indicate of the use of HE at this site.

**Figure 4-7**
**Kirtland Target NDIA, Geophysics Data**

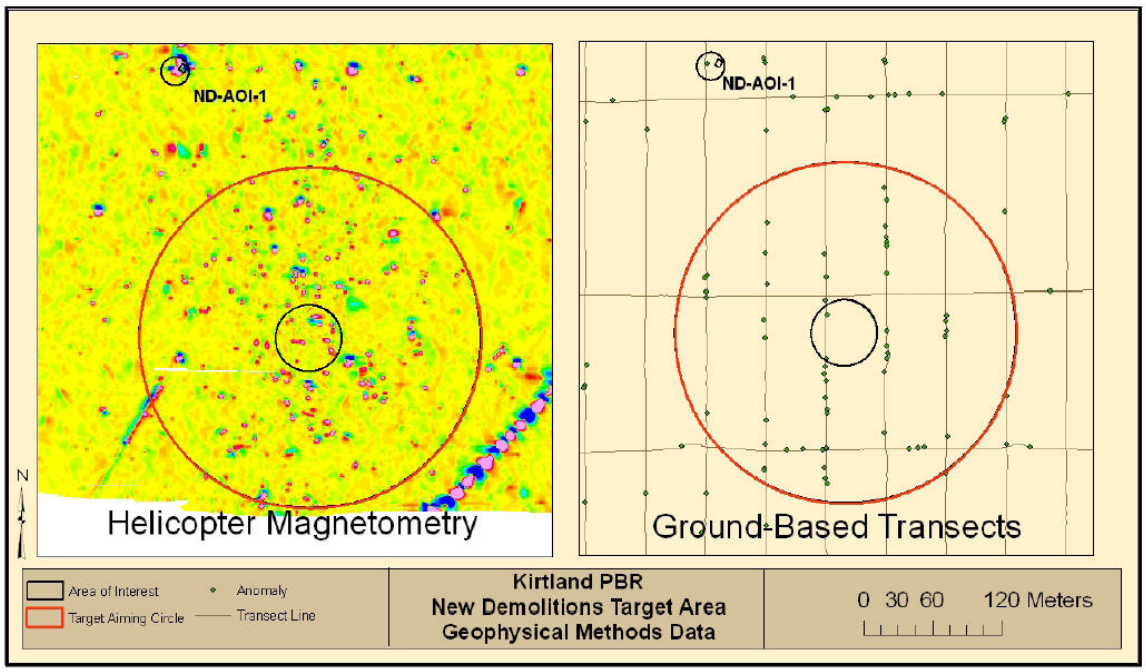


Source: ESTCP (2007a)

### *Additional Areas*

Eleven additional AOIs were identified at the Kirtland site, nine of them in the southern portion of the study area and two in the northern portion near Target N2. The archival search report did not indicate any munitions-related activities in these areas, and subsequent surveys found all but one of these AOIs to be building foundations, animal burrows, or other areas with no evidence of ordnance use. The one exception was the potential bull's-eye target described in Section 3.7.9,

which was found to contain a small number of anomalies: two rings of light-colored pebbles and a small amount of ordnance-related scrap. The revised CSM describes this as a possible aiming circle, with a medium confidence level. The site is located relatively close to a known target area just outside of the study area, and it is possible that this is the source of the ordnance-related scrap found.

### 4.2.4 Results: Victorville

***Target DBT Y***

Target DBT Y is described as a HE bombing target, and large craters were clearly shown using both lidar and orthophotos. Helicopter and ground-based magnetometry and EMI found few anomalies at the site, and there was little evidence of munitions-related scrap. The revised CSM states that this is nevertheless consistent with potential HE use, which can leave few items large enough to result in either anomalies or visible scrap. The site has been the site of previous cleanup activities which may also account for the scarcity of items. Heavy-walled scrap indicative of HE use was found just outside of the dry lake bed near similar craters to those at the site.

***Target PBR 15***

Target PBR 15 is described as a bull's-eye target used for precision bombing practice. Orthophotos and lidar intensity imagery clearly showed the bull's eye rings. Concentrations of anomalies from both helicopter and ground-based magnetometry were found up to a circle of 1,000 feet in diameter surrounding the target. The lack of cratering at the target supported the conclusion that the target was used for practice bombing.

Figure 4-8 shows the ground magnetometry transect data as filtered for geologic noise. Target PBR 15 is clearly visible in the southeast portion of the site. Target DBT Y is faintly visible.

**Figure 4-8**
**Victorville Filtered Geophysics Data**

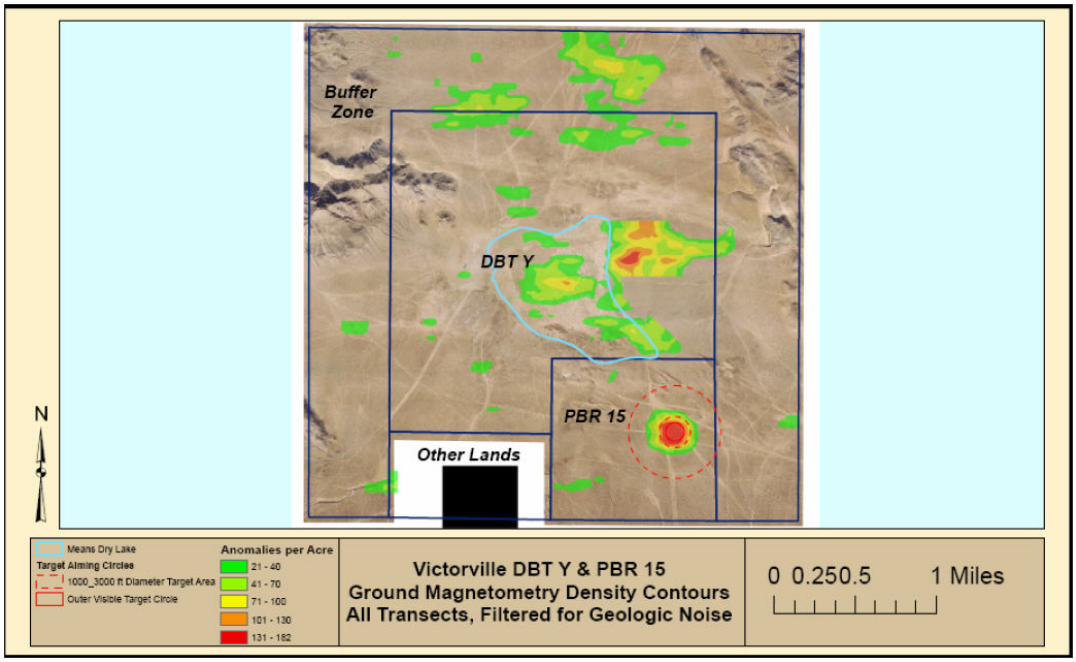


Source: ESTCP (2007b)

### *Additional AOIs*

Figure 4-9 shows the additional AOIs identified at the Victorville site. All but the craters west of the dry lake bed were identified based on the magnetometry and EMI surveys. Lidar data showed a number of apparent craters west of the dry lake bed, and ESTCP conducted site reconnaissance of some of these features (labeled in the revised CSM as DBTY-AOI-1). The presence of heavy-walled ordnance frag confirmed that some of these features were craters from HEs. However, the small number of craters found suggested that these craters were from pilot error rather than a separate target. Others features to the far west in this area were identified as mining prospect pits or large boulder formations. The other AOIs were examined with ground-based magnetometry and EMI sensing, and were determined not to be ordnance-related.

**Figure 4-9**
**Victorville Helicopter Magnetometry Density Grid**

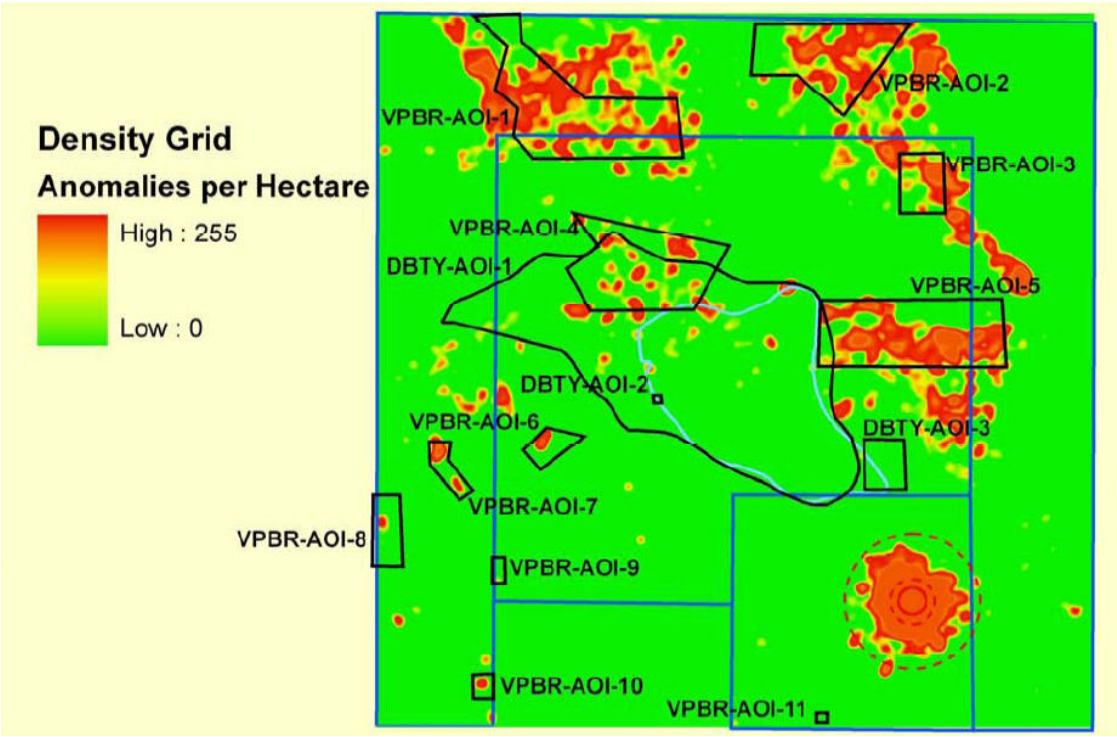


Source: ESTCP (2007b)

### 4.2.5 Findings and Conclusions

Examination of the lidar and orthophoto data in light of the subsequent activities at the two sites led to the following findings and conclusions:

- Lidar and orthophotos located all of the major target features. The general locations of these targets were consistent between the lidar and orthophoto data and that of the other technologies used.

- Lidar and orthophotos did not locate two ordnance-related areas associated with Kirtland Target N3, presumably because these areas did not show ground disturbances. These areas were detected using all of the magnetometry platforms, and were verified through intrusive investigation. This result points out a limitation of these light-based technologies: because they do not direct ordnance components directly, they can miss areas of munitions use that do not leave evidence on the ground surface. Consequently, use of lidar and orthophotos should be supplemented with other technologies where appropriate.

- Lidar and orthophotos tended to understate the extent of distribution of ordnance-related scrap at the Kirtland site. Ordnance-related scrap continued to be found in most of the areas of 100% coverage and intrusive investigation, well past what would have been estimated as conservative boundaries of the features using the lidar and orthophoto data. The reason for this wide distribution of ordnance scrap is not known. Because no intrusive sampling was done at the Victorville site, it is unknown whether this pattern would be found at the targets there. It is possible that methods could be developed to better extrapolate from features shown in lidar to the actual extent of ordnance-related scrap. However, this would require the examination of both lidar and orthophoto as well as validation data from a wider variety of sites.

- Lidar and orthophotos found targets using berms or craters that would not have been inferred from helicopter magnetometry data alone, including the main target ring at Kirtland Target N3 and Victorville Target DBT Y.

## 4.3 DATA ANALYSIS, INTERPRETATION, AND EVALUATION

### 4.3.1 Correlations with Operating Parameters and Required Performance Specifications

Of the operating parameters tested, lidar and orthophoto data density showed the strongest correlation with operational results. Of the two orthophoto pixel sizes tested, the 10 cm pixel images clearly outperformed the 20 cm images, allowing the detection of objects at or below 1 m in size. This is a significant result for two reasons: first, because the smaller pixel size is more expensive to acquire, and second, because both 10 cm and 20 cm pixel orthophotos are more dense than conventionally available orthophotography, which very seldom has pixel sizes smaller than 32 cm (1 foot).

Lidar data density clearly affected the detection of smaller craters. This effect was not as strong for the bombing targets, which were well detected using all but the lowest-density lidar data collected of 1.5 pts/ $m^2$. At this level, bull's-eye target rings began to be missed.

At future sites where detection of large features such as bombing targets is the principle objective, lidar data densities would not need to be as high as for reliable detection of craters. Nevertheless, additional lidar density should probably be acquired if the project budget and the vendor's equipment allow, since additional lidar density will help to define features more clearly. Additionally, this demonstration showed that lidar data density varied considerably over the project area. Increasing overall lidar density is one way to compensate for the possibility that some areas will be less dense than planned.

Data from this demonstration also suggests that if possible, increased lidar density should be acquired through use of faster sensors or lower flight elevations, rather than through multiple

overlapping flights. This is because in areas of flightline overlap, current equipment characteristics and data processing methods exclude significant numbers of lidar points from the ground surface model. In areas with very sparse vegetation, the point classification problem can be eliminating by making surface models using all lidar points, however this approach cannot be used on vegetated sites. Further investigation is appropriate in this area.

Flight line orientation also had a detectable effect on detection of very shallow linear features, indicating that if a second lidar flight is collected in addition to the primary lidar/orthophoto flight, it should be flown perpendicular to the first flight.

### 4.3.2 Optimum Operating Conditions and Appropriate Uses of the Technologies

Results from the Kirtland and Victorville sites support the general premise of the WAA Pilot Program: lidar and orthophotos should be the first technologies to be deployed after completion of the archival search report and the initial CSM. At both sites, lidar and orthophotos were successful at revealing and verifying the broad picture of munitions use. Lidar, especially, was very successful at delineating targets and crater fields, as well as additional areas of interest that warranted investigation. Areas of interest that warranted further investigation were delineated. The two technologies complemented each other well, each providing data that the other did not. Since vendors generally offer the two technologies together, it makes sense to acquire both at future production sites.

At the Kirtland site, two AOIs were identified using magnetometry that were not detected using lidar and orthophotos, presumably because these areas did not leave any indications on the ground surface. This finding supports the WAA Pilot Program approach that lidar and orthophoto acquisition should be followed with technologies that directly detect ordnance components.

# 5.0 COST ASSESSMENT

## 5.1 COST REPORTING

Table 5-1 presents actual costs for the Kirtland and Victorville demonstration sites, and estimated costs for production sites of three different sizes. Cost figures for the 18,000-acre demonstration site are based on preliminary project costs for the Former Camp Beale site, acquired in 2006. The remaining figures are planning-level estimates, assessed to be accurate within +/- 20%. Per-acre costs for the Kirtland site were higher since four rather than two lidar flights were conducted, and one rather than two orthophoto sets were created. The Victorville configuration, with one lidar/orthophoto flight and one additional lidar-only flight, is considered representative for a production site where it is important to detect both targets and individual small features. The "50,000-acre production site" estimate is based on URS' previous experience and interviews with industry sources, and the "115,000-acre production site" estimate is based on a cost proposal made by URS for a site in the western US in fall 2005. All projects listed can be completed in less than one year; therefore, no discount factor has been applied to the figures.

**Table 5-1**
**Actual and Projected Costs**

| Project Parameters | Kirtland | Victorville | 18,000-acre Production Site | 50,000-acre Production Site | 115,000-acre Production Site |
|---|---|---|---|---|---|
| Project area size (acres) | 5,000 | 5,640 | 18,000 | 50,000 | 115,000 |
| Project area size (hectares) | 1,914 | 2,282 | 7,284 | 19,140 | 44,022 |
| **Lidar flights:** | | | | | |
| 300 m (Lidar only) | 2 | 1 | 1 | 1 | 1 |
| 450 m (Lidar and 10 cm pixel imagery) | 1 | 1 | 1 | 1 | 1 |
| 900 m (Lidar and 20 cm pixel imagery) | 1 | 0 | 0 | 0 | 0 |
| Total Lidar flights | 4 | 2 | 2 | 2 | 2 |
| Total Lidar point density (pts/m$^2$) | 20 | 8-10 | 8-10 | 8-10 | 8-10 |
| Orthophoto pixel size (cm) | 10 and 20 | 10 | 10 | 10 | 10 |
| **Costs (2006 $)** | | | | | |
| Fixed Costs | | | | | |
| Mob/demob | 15,600 | 23,100 | 21,800 | 30,000 | 45,000 |
| Planning/preparation | 15,000 | 9,200 | 15,000 | 15,000 | 20,000 |
| Project management | 15,000 | 10,000 | 25,000 | 40,000 | 100,000 |
| Site work | 0 | 0 | 0 | 0 | 0 |
| Equipment cost | 0 | 0 | 0 | 0 | 0 |
| Start-up and testing | 0 | 0 | 0 | 0 | 0 |
| Subtotal fixed costs | 45,600 | 42,300 | 61,800 | 85,000 | 165,000 |
| **Variable Costs (2006 $)** | | | | | |
| Data acquisition | 39,900 | 34,100 | 85,300 | 160,000 | 355,000 |
| Data processing | 45,800 | 35,200 | 102,900 | 250,000 | 575,000 |
| Data analysis and GIS products | 94,300 | 30,000 | 68,100 | 150,000 | 220,000 |
| Data reporting and documentation | 13,600 | 8,500 | 12,000 | 15,000 | 25,000 |
| Materials and consumables | 1,500 | 1,000 | 1,500 | 5,000 | 10,000 |
| Other direct costs | 0 | 0 | 0 | 0 | 0 |
| Subtotal variable costs | 195,100 | 108,800 | 269,800 | 580,000 | 1,185,000 |
| **Total project cost (2006 $)** | **240,700** | **151,100** | **331,679** | **665,000** | **1,350,000** |
| **Total per/acre cost (2006 $)** | **48.1** | **26.8** | **18.43** | **13.3** | **11.7** |
| **Total per/hectare cost (2006 $)** | **125.8** | **66.2** | **45.53** | **34.7** | **30.7** |

## 5.2 COST ANALYSIS

### 5.2.1 Cost drivers

The major cost drivers for the two demonstration sites were:

- **Lidar data density required.** For the Kirtland site, four lidar flights were conducted; two concurrently with digital imagery collection, and two lidar-only flights. For the Victorville site, one lidar/orthophoto flight and one lidar-only flight were conducted.

- **Orthophoto data density required.** For the Kirtland site, two sets of digital images were collected, and orthophotos were created at 10 cm and 20 cm pixel sizes. For the Victorville site, only 10 cm pixel size was collected.

- **Accuracy and precision requirements.** A higher level of survey control was needed at the Kirtland PBR site than for production sites, in order to verify the accuracy and precision of the lidar and orthophoto data and to confirm that data could be successfully integrated with the other technologies demonstrated. It is estimated that during production projects fewer survey control points and vertical control structures would be needed.

- **Site location/logistics.** The Kirtland PBR site location affected project costs both positively and negatively. Positive effects were that the Double Eagle Airport was immediately adjacent to the project site and the helicopter vendor used was based at this site. These factors lowered mobilization and equipment rental costs and eliminated fees for fuel transport. Negative factors were that the high level of air traffic at the airport required hiring a second pilot. In addition to the additional labor cost, the additional weight resulted in higher fuel costs. At the Victorville site, fuel had to be transported to the site and helicopter flight times were longer, creating somewhat higher site-related costs than for Kirtland.

In addition to the cost drivers listed above, costs for production sites will be affected by the following additional factors:

- **Site size.** Larger sites achieve cost savings through amortization of fixed costs such as mobilization and project planning, as well as through increased efficiency in data acquisition and processing.

- **Vegetation conditions.** Highly vegetated sites will have higher costs due to the requirement for additional lidar passes to achieve sufficient density of points reaching the ground surface.

- **Permitting and site access constraints.** DoD sites with sensitive, high-security areas may have higher costs. However, such conditions would typically affect only pre-flight planning and equipment mobilization costs rather than data acquisition, processing and analysis costs. Sites with environmental constraints do not normally impose significantly higher costs for lidar and orthophotography, since the airborne nature of the technologies does not typically affect sensitive species or environments.

### 5.2.2 Cost Sensitivities and Additional Potential Savings

Additional savings could be realized through either of the following methods:

- **Acquiring orthophotography with a larger pixel size.** The cost of acquiring and processing orthophotography rises dramatically for smaller pixel sizes, and acquiring orthophotos at 20 cm pixel size rather than 10 cm would reduce the data acquisition and processing costs by 30 to 35%. The utility of such photos would be lower since their resolution will not allow discrimination of smaller features. Nevertheless, this may be an appropriate solution for sites where orthophotography is inherently less useful, such as sites with heavy tree cover. At such sites, pre-existing orthophotography from other sources may be acceptable if its positional accuracy can be verified.

- **Acquiring lower-density lidar data.** Eliminating the assumed second lidar flight, and thus only collecting lidar with the 10 cm orthophoto imagery, would reduce costs by 25 to 30%. The ability of the resulting lidar data set to discriminate features would be reduced; however, this might be appropriate if the lidar data was to be used only to discriminate large features such as bombing targets or roads, rather than smaller features such as craters. Alternatively, DoD could specify use of a faster lidar sensor, which could meet lidar data density requirements from a single pass.

Some additional cost savings could potentially be achieved by establishing Service- or DoD-wide standards for data acquisition, GIS data product creation, data delivery formats, and project reporting.

## 5.3 COST COMPARISON

Cost comparisons with the other innovative technologies demonstrated as part of the ESTCP WAA Pilot Program will be made in the Final Report for the WAA Pilot Program.

# 6.0 IMPLEMENTATION ISSUES

## 6.1 ENVIRONMENTAL CHECKLIST

No environmental regulations applied to the demonstration and no permits were required.

## 6.2 OTHER REGULATORY ISSUES

Both lidar and orthophotography are in wide commercial use. Within the United States, no regulatory restrictions are known that would impede the wide use of either technology. Outside of the United States, use of advanced IMU equipment may be restricted in certain countries. The IMU used in lidar systems is military dual use technology and international use requires a permit under the International Traffic in Arms Regulations (22 CFR 120-130). Additionally, some countries impose a variety of restrictions on the acquisition, processing and subsequent use of lidar and orthophoto data collected within their borders, particularly in border or military-use areas. Potential users of lidar in such situations should investigate such restrictions as part of project planning.

## 6.3 END-USER ISSUES

Both lidar and orthophotos are in wide commercial use and do not face substantial end-user issues.

# 7.0 REFERENCES

URS Corporation. 2001. *Quality Assurance Manual*. January.

———. 2005. Final Demonstration Plan, Project Number UX-0534, High Density LiDAR and Orthophotography in UXO Wide Area Assessment. July.

———. 2006a. Demonstration Plan Addendum for Victorville PBR Y Demonstration Site. January.

———. 2006b. Demonstration Plan Addendum for Former Camp Beale Demonstration Site. July.

Environmental Security Technology Certification Program. 2007a. Former Kirtland Precision Bombing Range, Conceptual Site Model. Draft Version 3.1. January.

———. 2007b. Victorville Precision Bombing Range: Demolition Bombing Target "Y" and Precision Bombing Range Target 15, Conceptual Site Model. Draft Version 2. January.

———. 2006a. Draft Reconnaissance Plan, Wide Area Assessment Pilot Program Demonstration at Victorville Precision Bombing Ranges Y & 15, CA. September.

———. 2006b. Draft Validation Plan, Wide Area Assessment Pilot Program Demonstration at Former Kirtland Precision Bombing Range, NM. January.

# APPENDIX A

# LIDAR AND ORTHOPHOTO POSITIONAL ACCURACY RESULTS

# APPENDIX B

# COMBINING LIDAR DATA FROM MULTIPLE FLIGHTS

# APPENDIX C

# VARIATION IN LIDAR DATA DENSITY AND POTENTIAL EFFECT ON FEATURE IDENTIFICATION

# APPENDIX D

# GIS-BASED METHODS FOR CREATING GROUND SURFACE MODELS FROM LIDAR POINTS

# APPENDIX E

# AUTOMATION OF LIDAR DATA PROCESSING IN THE ESRI GIS ENVIRONMENT

# APPENDIX F

# ANALYTICAL METHODS SUPPORTING EXPERIMENTAL DESIGN

# APPENDIX G

# QUALITY ASSURANCE PROJECT PLAN

# APPENDIX H

# HEALTH AND SAFETY PLAN

# APPENDIX I

# POINTS OF CONTACT